Journal of

Robotics, Automation, and Electronics Engineering

Vol. 3, No. 1, March 2025

ISSN 3025-3780(online)
ISSN 3025-4590(printed)

Journal of

Robotics, Automation, and Electronics Engineering

Vol. 3, No. 1, March 2025

JRAEE REVIEWERS

ISSN 3025-3780(online)
ISSN 3025-4590(printed)

ISSN 3025-3780(online)
ISSN 3025-4590(printed)

Journal of

Robotics, Automation, and Electronics Engineering

Vol. 3, No. 1, March 2025

TABLE OF CONTENTENS

JRAEE

Journal of Robotics, Automation, and Electronics Engineering
Vol. 3, No. 1, 2025, pp. 112-123
e-ISSN 3025-3780
https://journal.uny.ac.id/v3/jraee

Design and Implementation Fuzzy Tsukamoto-Based Temperature and Humidity Control for Aeroponic Pakcoy Cultivation

Fitria Alysa Yasmin[a,1], Purno Tri Aji[b,2,*]

[a, b]Dept. of Electrical and Electronic Engineering, Vocational Faculty, Universitas Negeri Yogyakarta
[1]fitriaalysa.2019@student.uny.ac.id, [2]purno.tri@uny.ac.id
[*]Corresponding Author

ARTICLE INFO

Article History
Received 22 Oct 2024
Revised 29 Aug 2026
Accepted 31 Aug 2026

Keywords
Aeroponics;
Tsukamoto Fuzzy;
IoT (Internet of Things);
Blynk;
Pakcoy.

ABSTRACT

Aeroponics is a method of hydroponic cultivation where plant roots are suspended in the air and nutrients are supplied through misting. The temperature and humidity control system, along with the monitoring mechanism, was designed using an ESP32 microcontroller. Input was provided by DHT22 and HC-SR04 sensors, while actuators consisted of mini fans and pumps. Through the integration of an Internet of Things (IoT) system, data on temperature, humidity, and water levels in the nutrient solution were monitored via the Blynk IoT application on smartphones. The results indicated that the DHT22 sensor measured temperatures within the range of 25°C to 26°C, with an average error of 0.79, and humidity levels above 70%, with an average error of 0.34. The data were processed using the Tsukamoto fuzzy method to determine the pump operating time and the PWM value for the mini fan. The HC-SR04 sensor recorded water levels between 10.1 cm and 11.5 cm, with an average error of 0.46, which was displayed using red and green LED indicators. Monitoring via the Blynk IoT application successfully presented both data and graphs of sensor readings. The entire system functioned as designed, effectively maintaining the temperature and humidity in the aeroponic pakcoy plant watering container.

ABSTRAK

Aeroponik merupakan metode penanaman hidroponik dimana akar tanaman dibiarkan menjuntai di udara sehingga pemberian nutrisi dilakukan melalui pengabutan pada akar. Sistem pengendalian suhu, kelembapan, dan monitoring ini dirancang menggunakan mikrokontroler ESP32, dengan input dari sensor DHT22 dan HC-SR04, serta aktuator berupa mini fan dan pompa. Dengan menerapkan sistem Internet of Things (IoT), data suhu, kelembapan, dan ketinggian air larutan dapat ditampilkan pada aplikasi Blynk IoT yang tersedia di smartphone. Hasil penelitian menunjukkan bahwa sensor DHT22 mengukur suhu dalam rentang 25°C-26°C dengan rata-rata kesalahan 0.79, dan kelembapan di atas 70% dengan rata-rata kesalahan 0.34. Data tersebut diolah menggunakan metode fuzzy Tsukamoto untuk mengatur waktu operasi pompa dan nilai PWM pada mini fan. Sensor HC-SR04 mengukur ketinggian air dalam rentang 10.1

cm- 11.5 cm dengan rata-rata kesalahan 0.46, yang kemudian di tampilkan pada indikator LED merah dan hijau. Monitoring melalui aplikasi Blynk IoT berhasil menampilkan data dan grafik hasil pembacaan sensor. Keseluruhan sistem bekerja sesuai dengan perancangan untuk menjaga suhu dan kelembapan wadah penyiraman tanaman aeroponik pakcoy.

1. Introduction

Indonesia is one of the countries experiencing rapid development in the agricultural sector. As time goes by, the increasing population has led to more land being used for infrastructure development and urban expansion. Consequently, the shrinking of agricultural land has become one of the main issues in this field. The reduction in the area of agricultural land is now a factor driving farmers to switch to soil-less planting techniques such as hydroponics, aeroponics, and aquaponics. These methods are considered more efficient in addressing the issue of limited land for certain crops, as they require less space and emphasize optimal nutrient delivery. Hydroponics is a planting method that involves providing nutrients through the plant's roots by dissolving them in flowing water. Meanwhile, hydroponics is further divided into two categories: aquaponics and aeroponics. Aquaponics is a combined method of hydroponic techniques with the cultivation of aquatic organisms such as fish and shrimp. On the other hand, aeroponics is a hydro ponic method that utilizes nutrient mist to control temperature and humidity at the plant roots. In various aspects, aeroponics is considered to have a lower risk of crop failure due to its advantages, which include faster and more efficient plant growth, high oxygen content in the nutrient solution, and the ability to reduce the risk of plant diseases [1].

In aeroponics, roots are a crucial factor in plant growth, so watering is done continuously or intermittently at different intervals for each plant over several hours to maintain the moisture of the plant roots [2]. Automatic misting based on a timer, commonly used by aeroponic farmers, is considered less effective for misting roots; the amount of nutrients provided without considering temperature and humidity can alter the condition of plants in aeroponics. Plants experiencing nutrient excess or deficiency will have suboptimal growth results; for example, in pakcoy, problems may manifest as yellowing leaves or drying stems [3]. Therefore, misting with a fuzzy logic approach that considers the temperature and humidity of plant roots could serve as a solution to timer-based misting, helping to prevent fluctuations or extreme climate changes in the growing medium. Each plant has different ideal temperature and humidity values for its roots. Previous research using strawberries as the research object found the ideal root temperature to be between 14°C and 24°C and the ideal root humidity between 85% and 95%. Fuzzy logic-based automatic misting showed better results by taking plant and environmental factors into account [1].

For this study, the plants used were pakcoy grown outdoors, with ideal root temperature values of 20°C to 25°C and ideal root humidity values of 60% to 80% [4]. In outdoor pakcoy aeroponics, the misting duration runs continuously for 1-15 seconds every 15 minutes, with a harvest period of 45 days plus a seedling period of 6-8 days until the seedlings grow 4 leaves [4]. From the data obtained in previous research, it can be concluded that farmers need to pay attention to the root misting system and monitor the temperature and humidity conditions of plant roots, thus requiring automatic watering with temperature and humidity control for the roots. Additionally, the height of the nutrient solution used should also be monitored so that the pump can operate more effectively, as the pump used for misting can only draw water to a certain height. Due to the limited data regarding plant conditions that can serve as a reference for aeroponic farmers, monitoring for remote observation is necessary, including recording temperature and humidity values as well as nutrient solution height, which will facilitate real-time monitoring of plant conditions by farmers [5].

The problem-solving approach in this research is based on the results of previous studies related to controlling the temperature and humidity of plant roots in aeroponic systems and monitoring plant conditions. The solution to address the complexity of the plant environment caused by climate fluctuations in the aeroponic planting method involves an approach derived from prior research. This approach includes automatic watering utilizing fuzzy logic as the main method in this study for automated plant irrigation control. The use of fuzzy logic in this research functions to manage uncertainties in sensor data by classifying it based on environmental changes to enhance plant quality. Classification in fuzzy logic is essential to achieve sufficient accuracy in nutrient misting at the plant roots to avoid excess or deficiency.

ISSN 3025-3780 (online)
ISSN 3025-4590 (printed)

The actuators in the control system generated by fuzzy logic are a DC jet pump and a mini fan, which function to regulate temperature and humidity within the growing box. Temperature and humidity values are obtained from the DHT-22 sensor, while the height of the nutrient solution is measured using the HC-SR04 sensor. Monitoring is done using an IoT (Internet of Things) approach with the ESP32 as the microcontroller, which can connect to Wi-Fi to transmit data obtained from the sensors to electronic devices capable of sending data over the internet [5]. This makes it easier for farmers to monitor plant conditions remotely using a smartphone integrated with the internet.

2. Related Work

Aeroponic cultivation has become one of the most promising technologies in modern agriculture because it enables plants to grow without soil while significantly reducing water and nutrient consumption. In aeroponic systems, plant roots are suspended in air and periodically sprayed with nutrient-rich mist, allowing efficient oxygen absorption and accelerating plant growth. Previous studies have demonstrated that aeroponic cultivation offers higher productivity than conventional soil-based farming while requiring considerably less cultivation area [6]. These advantages make aeroponic systems particularly suitable for urban farming and controlled environment agriculture. Despite these benefits, maintaining optimal environmental conditions remains one of the primary challenges in aeroponic cultivation. Temperature and relative humidity directly influence plant transpiration, nutrient uptake, photosynthetic efficiency, and overall crop development [7]. Environmental fluctuations caused by weather variations or greenhouse conditions may reduce plant growth and increase the risk of disease. Consequently, automatic environmental control systems have become an important component of smart agriculture.

The rapid advancement of the Internet of Things (IoT) has significantly improved the capability of environmental monitoring systems. IoT-based agricultural platforms integrate environmental sensors, wireless communication, cloud computing, and embedded controllers to provide real-time monitoring and remote management of cultivation systems. Sensors continuously collect environmental data that are processed by microcontrollers before being transmitted to web or mobile applications for visualization and analysis. Such systems improve operational efficiency while reducing labor requirements.

Although IoT technology provides reliable monitoring capabilities, intelligent decision-making algorithms are required to regulate environmental conditions automatically. Conventional threshold-based controllers generally operate using fixed setpoints. These methods are simple to implement but often produce oscillatory actuator behavior because they cannot adequately represent the nonlinear characteristics of agricultural environments. As environmental variables continuously fluctuate, threshold-based control frequently causes excessive actuator switching, reducing both system stability and component lifetime.

Artificial intelligence techniques have therefore become increasingly popular in smart agriculture. Among these techniques, fuzzy logic has attracted considerable attention because it effectively represents human reasoning without requiring complex mathematical models. Instead of relying on precise equations, fuzzy logic utilizes linguistic variables and expert knowledge to describe system behavior under uncertain conditions. This characteristic makes fuzzy logic particularly suitable for environmental control applications where multiple variables interact simultaneously. Several fuzzy inference methods have been proposed, including Mamdani, Sugeno, and Tsukamoto. The Mamdani method is widely recognized for its intuitive rule representation but generally requires computationally intensive defuzzification procedures [8]. The Sugeno method offers computational efficiency by producing mathematical output functions, making it suitable for optimization and adaptive control applications [9]. In contrast, the Tsukamoto method employs monotonic membership functions that generate crisp outputs from each inference rule, allowing efficient real-time implementation on embedded microcontrollers while maintaining relatively low computational complexity [10].

Previous studies have successfully applied fuzzy logic to greenhouse climate regulation, irrigation scheduling, hydroponic nutrient management, and smart farming systems. Most reported improvements include better environmental stability, reduced water consumption, and increased crop productivity compared with manual operation. However, many existing studies primarily focus on monitoring environmental parameters rather than implementing adaptive automatic control. Furthermore, several systems utilize only a single environmental variable, limiting their capability to respond to dynamic cultivation conditions. Recent developments in low-cost embedded systems have enabled the integration of fuzzy controllers into compact agricultural platforms. Microcontrollers such as the ESP32 provide sufficient processing capability to perform real-time fuzzy inference while simultaneously managing multiple sensors and actuators. Combined with wireless connectivity, these platforms offer affordable solutions for intelligent agriculture, particularly for small-scale farmers and educational research laboratories. Although numerous studies have investigated fuzzy-based environmental control, relatively few have implemented the Fuzzy Tsukamoto algorithm for simultaneous temperature and humidity regulation in aeroponic Pakcoy cultivation. Most previous systems emphasize greenhouse applications or hydroponic cultivation rather than compact aeroponic environments. In addition, comprehensive evaluations involving sensor accuracy, control performance, and prototype implementation remain limited.

To address these limitations, this study proposes an intelligent environmental control system that combines temperature and humidity sensing with the Fuzzy Tsukamoto inference algorithm in an embedded ESP32 platform. Unlike conventional threshold-based approaches, the proposed system continuously adapts actuator operation according to changing environmental conditions, enabling more stable cultivation environments and reducing manual intervention. The integration of real-time sensing, intelligent decision making, and automatic environmental regulation represents the primary contribution of this work toward low-cost smart agriculture systems.

3. Method

This research uses the R&D (Research and Development) method to enhance knowledge and develop existing products. This method also provides an understanding of research involving hardware and software through a needs analysis procedure, followed by the development phase and concluded with evaluation. According to Borg and Gall, the meaning of this research model is a process used to develop and validate educational products [11].

3.1 Schematic Diagram

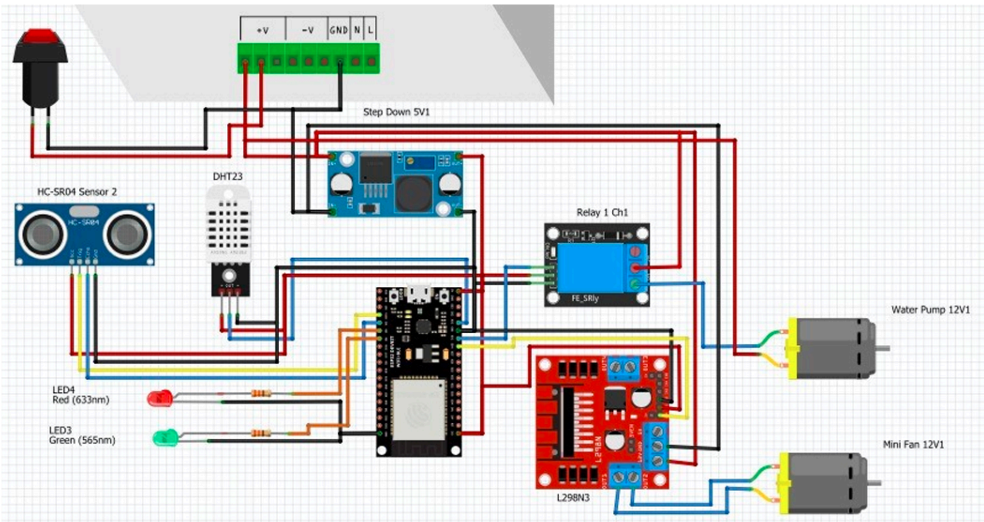

Fig.1 Schematic Diagram

The electronic circuit was designed based on the functional requirements of each component to support the automated monitoring and control processes. The system is powered by a 12 V power supply equipped with a switch button that functions as the main power switch to turn the system on and off. The output voltage from the power supply is distributed directly to the L298N motor driver through its 12 V and GND terminals and to a 12 V-to-5 V step-down converter via the Vin (+) and Vin (−) terminals to provide a regulated 5 V supply for components requiring lower operating voltages.

The ESP32 microcontroller serves as the central controller, coordinating data acquisition from the sensors and controlling all actuators. The ESP32 interfaces with a single-channel relay module, L298N motor driver, red and green indicator LEDs, DHT22 temperature and humidity sensor, and HC-SR04 ultrasonic sensor through dedicated GPIO pins according to their respective functions.

The DHT22 sensor is employed to measure ambient temperature and humidity. It is connected to the ESP32 with the VCC pin supplied by 5 V, the GND pin connected to ground, and the data pin connected to GPIO 13. Meanwhile, the HC-SR04 ultrasonic sensor is used for distance measurement and is connected through the 3.3 V, GND, TRIG (GPIO 15), and ECHO (GPIO 2) pins.

 ISSN 3025-3780 (online)
ISSN 3025-4590 (printed)

Actuator control is performed using the L298N motor driver, which receives control signals from GPIO 14 of the ESP32. The driver operates a mini fan connected to the OUT1 and OUT2 terminals of the L298N. Additionally, the single-channel relay module is connected to the 3.3 V, GND, and GPIO 12 pins of the ESP32 to control electrical loads according to the predefined control logic implemented in the software.

All hardware components are integrated into a single electronic system, enabling coordinated operation from sensor data acquisition and processing by the ESP32 to automatic actuator control based on real-time environmental conditions. The detailed schematic diagram is shown in Figure 1.

3.2 Voltage Flow Design

The voltage flow design is used to determine the voltage pathway starting from the 12V 5A power supply. Based on the flowchart created, the voltage is divided into two pathways: 12V to power the L298N motor driver for the 12V mini fan and the DC pump. Meanwhile, the voltage is stepped down to produce 5V for the ESP32 microcontroller, which will supply power to the DHT22 sensor, HC SR04 sensor, green and red LED indicators, and a 1-channel relay. This voltage flow design serves to map the components that require 5V power, thus minimizing the risk of short circuits. The voltage block diagram is presented in Figure 2.

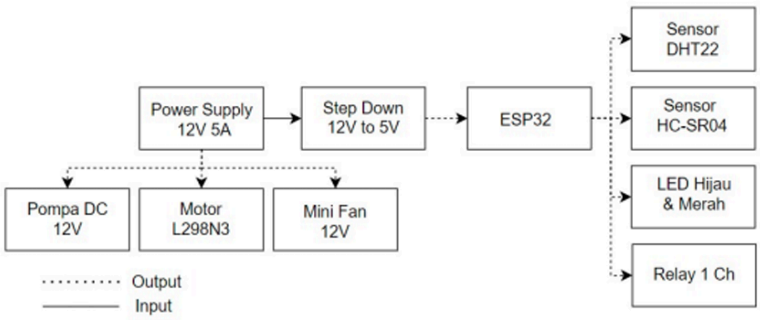

Fig.2 Voltage Block Diagram

3.3 3D Design of the Aeroponic Prototype

The prototype of the aeroponic temperature and humidity control system was designed using Tinkercad to create a three-dimensional (3D) visualization as a reference for the hardware development process. The prototype consists of two separate compartments with distinct functions. The first compartment serves as the aeroponic growing chamber and is constructed from transparent material to facilitate visual observation of the nutrient spraying process on the plant roots. The nutrient delivery system employs spray nozzles positioned beneath the suspended roots, with one nozzle assigned to each plant to ensure uniform nutrient atomization. In addition, a 12 V mini fan and a DHT22 temperature and humidity sensor are installed inside the growing chamber to support environmental monitoring and climate control. Figure 3 shows the 3D design of the proposed aeroponic system.

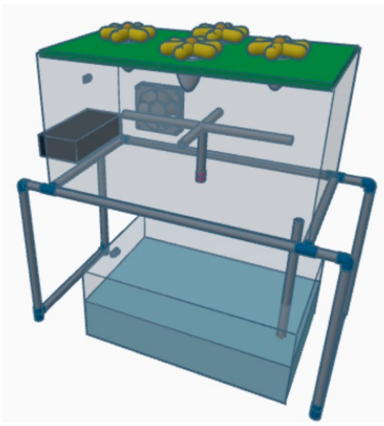

Fig.3 3D Design of Proposed Aeroponic System

The second compartment functions as the nutrient solution reservoir. After the nutrient solution is sprayed onto the plant roots in the growing chamber, the excess solution is returned to the reservoir through a recirculation system, preventing nutrient accumulation within the cultivation chamber. An HC-SR04 ultrasonic sensor is installed in the reservoir to monitor the nutrient solution level continuously. Meanwhile, the electronic control unit, which houses the microcontroller and supporting electronic components, is placed in a separate enclosure outside the aeroponic system to protect it from water splashes generated during the spraying process.

The separation of the growing chamber, nutrient reservoir, and electronic control unit was intentionally implemented to improve system reliability and measurement accuracy. Positioning the DHT22 sensor inside the growing chamber enables accurate measurements of the environmental temperature and humidity surrounding the plant roots, thereby providing reliable input data for the fuzzy logic controller. Similarly, placing the HC-SR04 sensor in the nutrient reservoir prevents exposure to the mist generated by the spray nozzles, reducing the risk of measurement errors and potential sensor damage. The prototype is supported by a 35 cm-high PVC frame with a table-like structure, while the DC water pump is positioned adjacent to the electronic control unit to facilitate nutrient solution delivery to the spraying system.

3.4 Tsukamoto Fuzzy

The method used is the Tsukamoto fuzzy method. The selection of the Tsukamoto method is based on the consideration that the Mamdani and Sugeno methods have been used in previous re search, making Tsukamoto a choice for further research development. The Tsukamoto fuzzy method also has advantages in terms of simplicity of objective selection using IF-THEN rules, as it produces linear outputs, which facilitates implementation and understanding. This differs from decision making with classical logic, which emphasizes true or false values (0 or 1). Fuzzy logic makes decisions based on membership to measure the value of a statement or action.

Table 1. Temperature and Humidity Membership Function Intervals

Variable	Interval
Temperature – Cold	[15, 15, 18, 21]
Temperature – Normal	[20, 22.5, 25]
Temperature – Hot	[24, 28, 32, 32]
Humidity – Dry	[0, 0, 32.5, 65]
Humidity – Humid	[60, 72.5, 85]
Humidity – Wet	[80, 100, 100]

Table 1 presents the fuzzy membership functions used to transform numerical temperature and humidity measurements into linguistic variables during the fuzzification process. Each input variable is represented by three overlapping fuzzy sets, enabling smooth transitions between adjacent membership functions and providing more flexible decision-making than conventional threshold-based methods.

For the temperature variable, three fuzzy sets are defined: Cold, Normal, and Hot. The Cold membership function is represented by the interval [15, 15, 18, 21], indicating that temperatures below 15 °C have full membership ($\mu = 1$), while the membership value gradually decreases to zero at 21 °C. The Normal fuzzy set is defined by the interval [20, 22.5, 25], where the membership value increases from 20 °C, reaches its maximum at 22.5 °C, and decreases to zero at 25 °C. Meanwhile, the Hot fuzzy set is represented by the interval [24, 28, 32, 32], where the membership value begins to increase at 24 °C, reaches full membership at 28 °C, and remains fully active up to 32 °C.

Similarly, the humidity variable is divided into three fuzzy sets: Dry, Humid, and Wet. The Dry membership function is defined by the interval [0, 0, 32.5, 65], indicating high membership values at low humidity levels that gradually decrease to zero at 65%. The Humid fuzzy set is represented by the interval [60, 72.5, 85], with the highest membership value occurring at 72.5%, corresponding to the optimal environmental humidity for the aeroponic system. The Wet membership function is defined by the interval [80, 100, 100], where the membership value increases from 80% and reaches full membership at 100% relative humidity. The temperature and moisture level membership functions are shown in Figure 4 and Figure 5.

Journal of Robotics, Automation, and Electronics Engineering
Vol. 3, No. 1, 2025, pp. 112-123
ISSN 3025-3780 (online)
ISSN 3025-4590 (printed)

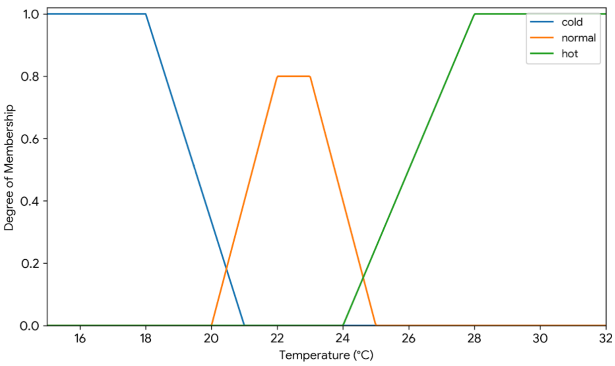

Fig. 4 Temperature Membership Functions

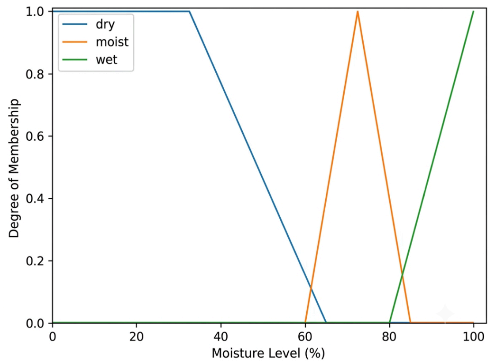

Fig.5 Moisture Level Membership Functions

The overlap between adjacent fuzzy sets allows a single sensor reading to simultaneously belong to multiple linguistic categories with different degrees of membership. For example, a temperature of 20.5 °C may partially belong to both the Cold and Normal fuzzy sets. This overlapping characteristic is one of the primary advantages of fuzzy logic, as it effectively represents gradual transitions observed in real-world environments and avoids abrupt changes in system responses.

Overall, the fuzzy intervals defined in Table 1 serve as the basis for the fuzzification process, in which crisp sensor measurements are converted into linguistic variables. These linguistic values are subsequently processed during the fuzzy inference stage to determine the appropriate control actions, such as regulating the cooling fan and nutrient spraying system, thereby maintaining optimal environmental conditions within the aeroponic cultivation system.

Table 2. Spraying Duration Based on Temperature and Humidity Conditions

Rule	Input	Spraying Duration (s)
1	Temperature **Cold** & Humidity **Dry**	Fast (5 s)
2	Temperature **Cold** & Humidity **Humid**	Normal (10 s)
3	Temperature **Cold** & Humidity **Wet**	Slow (15 s)
4	Temperature **Normal** & Humidity **Dry**	Normal (10 s)
5	Temperature **Normal** & Humidity **Humid**	Slow (15 s)
6	Temperature **Normal** & Humidity **Wet**	Slow (15 s)
7	Temperature **Hot** & Humidity **Dry**	Slow (15 s)
8	Temperature **Hot** & Humidity **Humid**	Normal (10 s)
9	Temperature **Hot** & Humidity **Wet**	Fast (5 s)

Table 2 presents the fuzzy rule base used by the proposed fuzzy inference system to determine the operating time of the nutrient spraying system and the rotational speed of the cooling fan based on the measured temperature and humidity conditions. The rule base consists of nine IF–THEN rules, which are derived from the combination of three temperature fuzzy sets (Cold, Normal, and Hot) and three humidity fuzzy sets (Dry, Humid, and Wet). Each rule produces two output variables: the spraying duration and the PWM value controlling the fan speed.

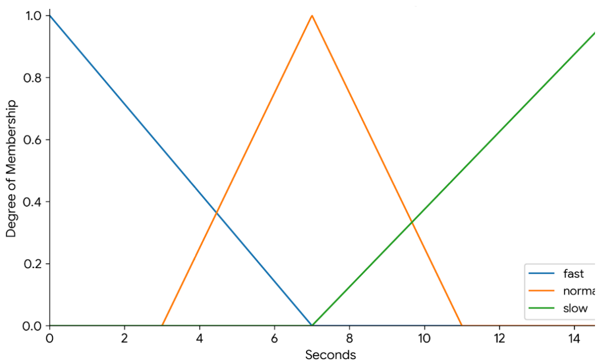

Fig.6 Spraying Duration Membership Function

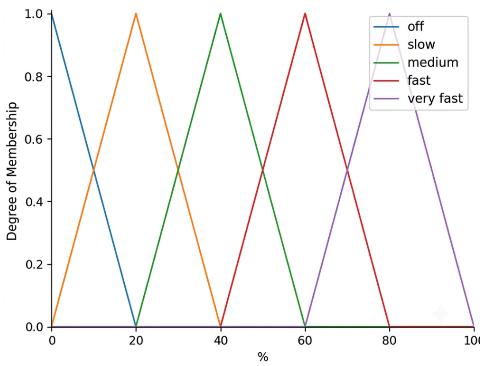

Fig.7 Membership Function for Fan Speed

The rules are formulated based on expert knowledge and the environmental requirements of the aeroponic cultivation system. When the environmental conditions are cold and dry (Rule 1), the spraying duration is set to Fast (5 s) while the fan operates at a Medium speed (PWM = 50). Under cold and humid conditions (Rule 2), the spraying duration is increased to Normal (10 s) while maintaining the same fan speed. If the environment is cold and wet (Rule 3), the spraying duration becomes Slow (15 s) and the fan speed is increased to High (PWM = 100) to reduce excessive humidity.

For normal temperature, the controller adjusts the outputs according to the humidity level. Under dry conditions (Rule 4), the spraying duration is Normal (10 s) and the fan is turned Off (PWM = 0). When the humidity is Humid (Rule 5), the spraying duration is increased to Slow (15 s) while the fan operates at a Medium speed (PWM = 50). Under Wet conditions (Rule 6), the spraying duration remains Slow (15 s), whereas the fan speed is increased to High (PWM = 100) to enhance air circulation.

When the temperature is classified as Hot, the controller prioritizes reducing the environmental temperature. Under dry conditions (Rule 7), the spraying duration is Slow (15 s) and the fan remains Off. When the humidity is Humid (Rule 8), the spraying duration is Normal (10 s) and the fan operates at a High speed (PWM = 100). Finally, under hot and wet conditions (Rule 9), the controller activates the Fast spraying duration (5 s) and the Very High fan speed (PWM = 255), representing the maximum cooling effort of the system. The spraying and fan speed duration membership function is presented in Figure 6 and Figure 7.

3.5 Monitoring Design

The monitoring design in this research uses the Blynk application with Wi-Fi connectivity. Based on the flowchart above, monitoring begins by initializing the ESP32, then connecting the ESP32 to the Blynk IoT application. If the connection is successful, the ESP32 will repeat the connection process. Once the ESP32 is connected to the Blynk IoT application, the device will operate, and the ESP32 will start reading the temperature and humidity from the DHT22 sensor, as well as the liquid level from the HC-SR04 sensor. Subsequently, the ESP32 will send the sensor data to the Blynk IoT application to be displayed on the Blynk IoT dashboard. The choice to use the Blynk application is based on several recommendations from previous studies, including the ease of access when switching devices, as the data remains stored in the cloud and can be accessed from other devices without losing information. Additionally, Blynk has a delay of around 3-5 seconds, allowing for real-time monitoring of sensor data. This application also supports stable connections with IoT devices like the ESP32 and features a user-friendly interface for monitoring and controlling devices. Monitoring is conducted by connecting the ESP32 to an Android device by entering the username and password provided in the Android personal hotspot.

4. Result and Discussion

4.1 Sensor Test

The temperature measurements obtained from the DHT22 sensor were compared with those recorded using a thermohygrometer as the reference instrument. The measurement difference ranged from 0.1 to 0.3 °C, with an average error of 0.79%. Based on the average percentage error, the sensor achieved an overall measurement accuracy of 99.21%, indicating good agreement with the reference instrument and demonstrating that the sensor is sufficiently reliable for temperature monitoring applications.

Table 3. Temperature Measurement Accuracy of the DHT22 Sensor

Minute	Sensor (°C)	Thermohygrometer (°C)	Difference	Error (%)
5	25.6	25.3	0.3	1.19
10	25.7	25.4	0.3	1.18
15	25.5	25.3	0.2	0.15
20	25.5	25.4	0.2	0.39
25	25.6	25.4	0.2	0.79
30	25.6	25.5	0.1	0.39
Average Error				**0.79**

The humidity measurements which presented in Table 3 obtained from the sensor were compared with those recorded using the thermohygrometer as the reference instrument. The measurement difference ranged from 0 to 0.9%RH, with an average error of 0.34%. Based on this result, the sensor achieved an overall measurement accuracy of 99.66%, indicating a high level of agreement with the reference instrument and demonstrating that the sensor is reliable for relative humidity monitoring. The temperature and humidity measurement accuracy of the DHT22 sensor are shown in table 3 and table 4.

Table 4. Humidity Measurement Accuracy of the DHT22 Sensor

ISSN 3025-3780 (online)
ISSN 3025-4590 (printed)

Minute	Sensor (%RH)	Thermohygrometer (%RH)	Difference	Error
5	99	99	0	0
10	98.9	98	0.9	0.91
15	98.4	98	0.4	0.40
20	98	98	0	0
25	97.5	97	0.5	0.51
30	97.2	97	0.2	0.20
Average error value				**0.34**

The ultrasonic sensor measurements were compared with those obtained using a ruler as the reference instrument. The measurement differences ranged from 0 to 1.0 cm, with an average error of 0.46 cm. Based on the average error, the sensor achieved an estimated measurement accuracy of 99.54%, indicating good agreement with the reference measurements and demonstrating that the ultrasonic sensor is suitable for distance monitoring applications. The distance measurement accuracy of the ultrasonic sensor can be found in table 5.

Table 5. Distance Measurement Accuracy of the Ultrasonic Sensor

Minute	Sensor (CM)	Ruler (CM)	Difference
5	11.5	10.8	0.7
10	11.1	10.5	0.6
15	11.1	10.1	1
20	10.5	10.1	0.4
25	10.1	10.1	0
30	10.1	10	0.1
Average error value			**0.46**

4.2 System Testing

The aeroponic prototype was designed with a multi-tier structure to maximize land-use efficiency while maintaining a compact cultivation system. The supporting frame was constructed from polyvinyl chloride (PVC) pipes, providing adequate structural strength and stability for the overall system. The completed aeroponic prototype is shown in Figure 8.

Fig.8 Implementation of the Aeroponic System Prototype

The testing of the entire system aims to determine whether there are any errors in the actuators during sensor readings and fuzzification. The temperature and humidity data collected are those displayed in the Blynk application, sent by the ESP32 microcontroller. The actuators involved are the pump and mini fan, which operate based on commands received after fuzzy processing. The testing was conducted over several days to achieve optimal results in accordance with the design. Below is the table of temperature and humidity control testing conducted over 105 minutes with 7 cycles of misting.

Table 6. Experimental Results of the Fuzzy Control System

Minute	Temperature (°C)	Humidity (%RH)	Fuzzy Pump (s)	Fuzzy Fan (PWM)
15	27.7	97.6	5	Very Fast (255)
30	27.5	87.7	10	Fast (100)

45	26.9	93.0	10	Fast (100)
60	26.8	96.1	10	Fast (100)
75	26.7	97.5	10	Fast (100)
90	26.4	98.2	10	Fast (100)
105	26.2	98.4	10	Fast (100)

Table 6 summarizes the performance of the proposed fuzzy control system over a 105-minute observation period. The recorded temperature gradually decreased from 27.7 °C to 26.2 °C, indicating that the control strategy effectively reduced the environmental temperature toward the desired operating range. Meanwhile, the relative humidity remained consistently high, fluctuating between 87.7%RH and 98.4%RH, which is suitable for aeroponic cultivation where high humidity is required to maintain healthy root development.

The fuzzy controller dynamically adjusted the spraying duration and fan speed according to the measured environmental conditions. At the beginning of the experiment (15 min), when both temperature and humidity were relatively high, the controller activated the pump for 5 s and operated the fan at the maximum PWM value (255) to rapidly stabilize the environment. As the temperature gradually decreased, the controller reduced the fan speed to PWM 100 while maintaining a 10 s spraying duration for the remainder of the experiment. This adaptive response demonstrates that the fuzzy inference system successfully modified the control outputs based on real-time sensor inputs rather than relying on fixed threshold values.

Overall, the experimental results indicate that the proposed fuzzy control algorithm provided stable environmental regulation by continuously adapting the pump operation and fan speed to changing temperature and humidity conditions. The gradual reduction in temperature without abrupt fluctuations suggests that the fuzzy-based control approach is effective for maintaining suitable environmental conditions in the aeroponic cultivation system.

4.3 Monitoring Testing

The purpose of the monitoring test is to check whether data is transmitted while the device is powered on, the Wi-Fi distance between the smartphone and the device, and to verify if the datastream readings are displayed while the device is running. The monitoring created in the Blynk application displays information in the form of temperature and humidity data obtained from the DHT22 sensor, as well as water level measurements using the HC-SR04 sensor, all presented in real-time. The programming developed commands the ESP32 to read and then send data from the sensors while the device is powered on.

Fig. 11. Aeroponic Monitoring Display

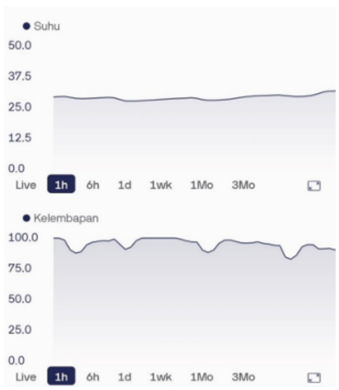

Fig.9 Aeroponic Monitoring Dashboard

The Blynk application successfully transmitted sensor data continuously while the device remained powered on. The monitoring system was able to display real-time environmental parameters, including temperature, relative humidity, and water level. In addition, the application provided graphical representations of the collected sensor data, enabling users to observe changes in environmental conditions over time. The monitoring results demonstrate that the developed system can reliably transmit, display, and visualize sensor data through the Blynk platform, as shown in Figure 9**.**

5. Conclusion

The proposed prototype of an automatic temperature and humidity control system for an aeroponic cultivation environment was successfully developed and implemented using a fuzzy logic controller. The experimental results demonstrated that the system was capable of maintaining the environmental temperature and humidity within the ranges required for optimal pakcoy growth under aeroponic conditions. The developed monitoring system, integrated with the Blynk IoT platform, successfully displayed real-time measurements of temperature (°C), relative humidity (%RH), and nutrient solution level (cm). Communication between the ESP32 microcontroller and the Blynk application exhibited an average latency of approximately 4 s, which was considered acceptable for real-time environmental monitoring.

Performance evaluation indicated that the proposed system achieved measurement accuracies of 99.2% for temperature, 99.6% for relative humidity, and 99.5% for nutrient solution level. Furthermore, the actuators, including the water pump and 12 V mini fan, operated according to the predefined fuzzy inference rules, enabling adaptive environmental control. During the experiment, the system successfully reduced the chamber temperature from 27.7 °C to 25.2 °C while maintaining the relative humidity within the range of 87%–90%, thereby creating favorable conditions for aeroponic cultivation.

In addition, the water-level indicator function operated as intended. The green LED was activated when the nutrient solution level exceeded 20 cm, whereas the red LED was illuminated when the water level dropped below 20 cm, indicating that the monitoring and warning functions performed correctly in accordance with the programmed control logic.

Author Contribution:

Fitria Alysa Yasmin: developed the hardware and software system, data collection, data analysis, interpretation of the results, and prepared the initial manuscript. Purno Tri Aji: preparation of the manuscript, and review and revision of the manuscript.

Funding:

This research received no external funding.

Acknowledgment:

The authors would like to thank all parties who provided support and assistance during the implementation of this research.

Conflicts of Interest:

The authors declare no conflict of interest.

References

[1] F. Suryatini, W. Purnomo, and M. Delistiani, “Pengendalian suhu dan kelembaban sistem aeroponik tanaman stroberi berbasis IoT menggunakan fuzzy logic,” JTRM (Jurnal Teknologi dan Rekayasa Manufaktur), vol. 2, no. 2, pp. 61–78, 2020, doi: 10.48182/jtrm.v2i2.20.

[2] Wulandari and N. W. Sumiar, “Pengembangan sistem pengaturan larutan nutrisi otomatis pada budidaya kentang aeroponik,” Jurnal Ilmu Komputer dan Agri-Informatika, vol. 8, no. 1, pp. 57–68, 2021, doi: 10.29244/jika.8.1.57-68.

[3] S. N. Iftitah, Teknologi Budidaya Tanaman Aeroponik. Pekanbaru, Indonesia: CV Bravo Press Indonesia, 2025.

[4] R. E. Putri, W. Fauzia, and D. Cherie, “Monitoring and control system development on IoT-based aeroponic growth of Pakcoy (Brassica rapa L.),” Jurnal Keteknikan Pertanian, vol. 11, no. 2, pp. 222–239, 2023, doi: 10.19028/jtep.011.2.222-239.

[5] P. D. B. Perteka, I. N. Piarsa, and K. S. Wibawa, "Sistem kontrol dan monitoring tanaman hidroponik aeroponik berbasis Internet of Things," Jurnal Ilmiah Merpati (Menara Penelitian Akademika Teknologi Informasi), vol. 8, no. 3, pp. 197–210, 2020, doi: 10.24843/JIM.2020.v08.i03.p05.

[6] M. Ihsan and Z. R. S. Elsi, "Assessment of plant growth in aeroponic systems integrated with smart farming compared to conventional methods," Jurnal Teknologi dan Ilmu Komputer Prima (JUTIKOMP), vol. 8, no. 1, pp. 40–52, 2025, doi: 10.34012/jutikomp.v8i1.7033.

[7] S.-W. Chu and T.-J. Wan, "Advancing sustainable agriculture through aeroponics: A critical review of integrated water–energy–nutrient management and environmental impact mitigation," Agriculture, vol. 16, no. 2, Art. no. 265, 2026, doi: 10.3390/agriculture16020265.

[8] R. Irawan, R. Hermawan, and I. S. Utami, "Mamdani method–based fuzzy inference system for determining the quality of Qur'an memorization," Journal of Mathematics Education and Science, vol. 9, no. 1, pp. 109–120, 2026, doi: 10.32665/james.v9i1.6183.

[9] T. Yulianto, S. Komariyah, and N. Ulfaniyah, "Application of fuzzy inference system by Sugeno method on estimating of salt production," AIP Conference Proceedings, vol. 1867, Art. no. 020039, 2017, doi: 10.1063/1.4994442.

[10] Y. P. Mahendra and R. F. Siahaan, "Penerapan metode fuzzy Tsukamoto dalam menentukan jumlah produksi opak pada Home Industri Tegar Jaya," Jurnal Pelita Ilmu Pendidikan (JPIP), vol. 2, no. 1, pp. 39–46, 2024, doi: 10.69688/jpip.v2i1.60.

[11] F. A. Slamet, Model Penelitian Pengembangan (R n D). Malang, Indonesia: Institut Agama Islam Sunan Kalijogo Malang, 2022.

JRAEE
Journal of Robotics, Automation, and Electronics Engineering
Vol. 3, No. 1, 2025, pp. 136-142
e-ISSN 3025-3780
https://journal.uny.ac.id/v3/jraee

Electrical System Design for the UG-22 Car for the Energy Efficient Car Competition

Muhammad Naufal Muafi[a,1], Sa'adilah Rosyadi[b,2,*]
[a, b]Dept. of Electrical and Electronic Engineering, Vocational Faculty, Universitas Negeri Yogyakarta
[1]muhammad0049ft.2020@student.uny.ac.id; [2]s.rosyadi@uny.ac.id
[*] Corresponding Author

ARTICLE INFO

Article History
Received 25 Oct 2024
Revised 29 Aug 2026
Accepted 31 Aug 2026

Keywords
Car;
Electrical System;
Efficient;
Grounding;
Resistance

ABSTRACT

This research examines the design and construction of the electrical system for the UG-22 car, the reduction of resistance in its electrical system, and the impact of these improvements on the car's results in the Energy Efficient Car Competition. The study describes the stages involved in designing and building the electrical system for the competition, as well as in optimizing the existing system, using the UG-22 car's electrical system as the object of study. Two optimization steps were taken: first, replacing the cable material with a type that has lower resistance; second, adding a grounding system to the car. The system design had to comply with the competition regulations, and the results show that optimizing the electrical system reduced electricity consumption in the UG-22 car. Cable resistance was reduced to 2.2 ohms, a decrease of 48.3%, and adding the grounding system reduced the voltage drop by 2 volts. As a result, electricity consumption was reduced by 49.71%, from 60 joules to 30.5 joules.

ABSTRAK

Penelitian ini bertujuan menguji rancang bangun sistem kelistrikan pada mobil UG-22, pengurangan resistansi pada sistem kelistrikan, dan dampak perbaikan sistem kelistrikan terhadap pencapaian dalam Kompetisi Mobil Hemat Energi. Penelitian ini mendeskripsikan tahapan dalam proses perancangan sistem kelistrikan mobil UG-22 untuk kompetisi mobil hemat energi, serta optimalisasi sistem dengan objek penelitian sistem kelistrikan mobil UG-22. Langkah yang diambil untuk mengoptimalkan sistem kelistrikan dengan mengganti material kabel dengan jenis yang memiliki resistansi rendah dan dengan menambahkan sistem *grounding* (pentanahan) pada mobil. Desain sistem kelistrikan harus memenuhi regulasi kompetisi, dan hasil penelitian menunjukkan bahwa optimalisasi sistem kelistrikan mampu mengurangi konsumsi listrik pada mobil UG-22. Resistansi pada kabel berkurang menjadi 2,2 ohm sebesar 48,3%, dan dampak penerapan *grounding* menunjukkan bahwa hal tersebut mengurangi penurunan tegangan (*voltage drop*) sebesar 2 volt. Selain itu, konsumsi listrik dapat ditekan sebesar 49,71% dari 60 joule menjadi 30,5 joule

1. Introduction

Vehicles rely on a complex network of systems that must work together optimally, with the electrical system being one of the most critical. Electricity plays an essential role in modern motor vehicles, which depend heavily on electrical current for many of their features. Vehicles are equipped with various vital electronic devices, for example, headlights are crucial for safety as they illuminate the road for drivers at night. Therefore, the placement and integration of these electronic components within the car must be both strategic and efficient.

The Energy Efficient Car Competition (*Kontes Mobil Hemat Energi, KMHE*) challenges teams to design, build, test, and drive vehicles that meet safety requirements while travelling the greatest possible distance on minimal energy. The competition is held in Indonesia by the Ministry of Energy and Mineral Resources and is included in the Puspresnas (National Achievement Center) agenda. It is intended to inspire students across Indonesia to innovate in response to future energy challenges. Vehicles entered in the 2022 competition were required to pass detailed technical inspections, for example checking that all bolts were properly tightened and that the doors locked correctly, before being allowed to continue to the race.

A poor-quality electrical system can reduce the responsiveness of sensors and other components, particularly in the ignition system, which depends heavily on the electric spark used for combustion. The effectiveness of a vehicle's ignition system is strongly influenced by its electricity supply. Ignition occurs when the spark plug produces a spark that ignites the compressed air–fuel mixture; it is measured in crankshaft degrees, both before and after Top Dead Center (TDC). The quality of the ignition timing must match the engine's specifications to achieve optimal performance, stronger ignition improves vehicle efficiency [1].

The electrical system of an energy-efficient car covers several circuits, broadly grouped into lighting and warning systems. The lighting system includes the headlights and daytime running lights, while the warning system includes the brake lights, turn signals, the horn, and the indicator and instrument lights. The electrical system plays a very important role in the vehicle, particularly as the main source of illumination when driving at night; it also signals other drivers when the car is turning or braking, and sounds the horn, all important elements of overall vehicle safety [1]. In the Energy Efficient Car Competition, teams must find ways to make both fuel consumption and electricity consumption as efficient as possible. This depends on selecting good-quality raw materials and using more advanced production techniques to create high-quality components. Vehicle weight is another factor that affects fuel consumption [3]: the heavier the car, the more power it requires. It is therefore important to identify the causes of high electricity consumption in the UG-22 car. One such cause is the quality of the cables used, a car's electrical system is the electronic circuit that manages every aspect of electricity in the vehicle. In other words, every component that uses electrical energy is part of the car's electrical system, and this system has a significant impact on fuel efficiency [2]. Because the Energy Efficient Car Competition is held every year, the Garuda UNY team must continually improve and re-evaluate its design. Problems have arisen from constraints in component and cable selection, and any redesign or rebuilding of the electrical system must comply with the rules and regulations issued for the 2022 competition.

2. Literature Review

2.1 The Energy-Efficient Car Competition (*Kontes Mobil Hemat Energi/KMHE*)

KMHE is a competition organized by the Ministry of Energy and Mineral Resources (ESDM) of the Republic of Indonesia, held since 2010 [4]. Its main objective is to encourage the advancement of energy-efficient car technology in Indonesia. In recent years, demand for energy-efficient cars has grown alongside increasing awareness of the importance of efficient, environmentally friendly energy use.

2.2 Basic Concepts of Electricity

Electricity is an essential component of any system used to produce an electric current that can serve as a power source. It can therefore be considered fundamental, for example an electric motorcycle cannot run without it. The following is a brief overview of the basic concepts of an electrical system [5]. This definition is not far removed from the one used in physics: the ability to do work. In everyday life, the energy used by machines and electronic devices is not the same as the energy needed by living things. Machines and electronic devices both require energy to function, but machines draw their energy from fuels such as gasoline, whereas electronic devices require energy in the form of electricity.

2.3 Cable Network

A cable network is a collection of individually insulated cables that connect the various components of a

ISSN 3025-3780 (online)
ISSN 3025-4590 (printed)

circuit. These cables are combined into a single unit to facilitate connections between the electrical components of a vehicle. Cables are the primary components of an electrical installation, channeling electrical energy to the equipment that uses it; they are also the most vulnerable component from the standpoint of electrical installation safety [6].

3. Research Method

This research is Research and Development (R&D), a method that produces a design or a product in a given field and evaluates its effectiveness. The study takes a quantitative approach, using numerical data obtained from measurements with a joule meter to determine how much electricity is consumed. This chapter describes the stages involved in designing and building the electrical system of the UG-22 car for the energy-efficient car competition. The stages used in the design process are shown in Fig. 1.

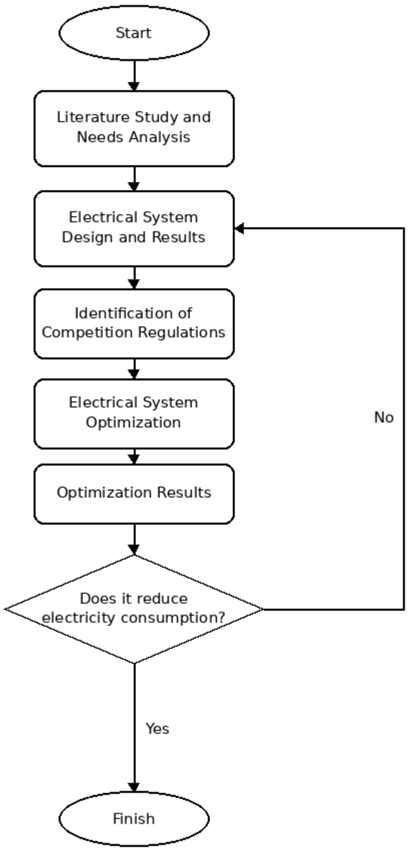

Fig.1 System flowchart design

3.1 Place and Time of Research

The research was conducted at the Faculty of Engineering, Yogyakarta State University (Universitas Negeri Yogyakarta), Karangmalang Campus, Yogyakarta. Its objective was the electrical system of the UG-22 car, with the goal of making it more efficient and achieving better results than in the previous year. The optimization was based on the team's 2021 competition data, which showed that the car's electrical system was still wasteful, particularly because of its cabling. The optimization work was carried out from January to September 2022 and then tested directly in the KMHE competition in October. During the project, the author had the opportunity to rebuild the UG-22's wiring in its entirety. Data gathered during vehicle testing and during the competition itself were used to develop this final thesis.

3.2 Research Procedures and Stages

- Requirement Analysis

Needs analysis is the initial stage carried out to determine the various requirements before designing the UG-22's electrical system. This analysis is based on the problems identified in the field and is carried out through a literature study.

ISSN 3025-3780 (online)
ISSN 3025-4590 (printed)

- System Design

Once the needs analysis is complete, the next step is to design the system. This stage produces a design that guides construction, ensuring that the system meets the desired specifications [8], and helps minimize errors during manufacturing. The design process includes planning the wiring layout and confirming that the system will function as expected once built.

System Flowchart: the first step in designing a car's electrical system is to map out the workflow of the system to be built. This is done by creating a system flowchart that describes the process and the sequence of steps needed to operate the system. The flowchart of the UG-22's electrical system for the energy-efficient car competition is shown in Fig. 2.

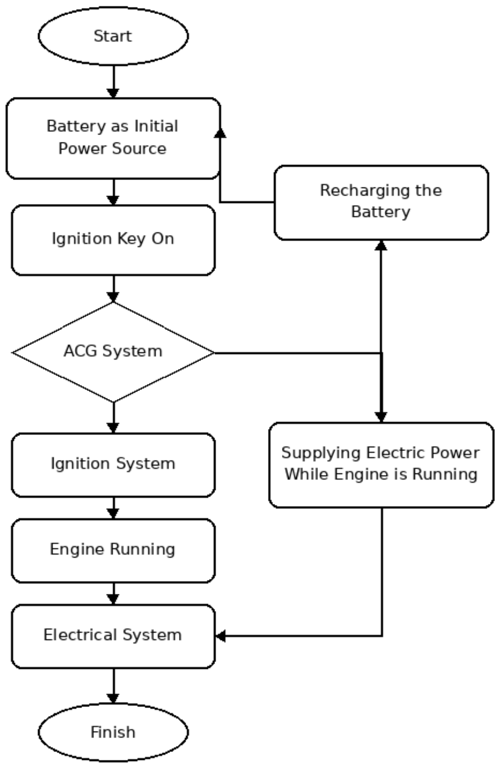

Fig.2 System flowchart design

- Electrical System Optimization

At this stage, the team addressed problems in the UG-22's electrical system by replacing its cables and adding a grounding system. These changes were intended to improve the efficiency of electricity consumption during the KMHE race and to ensure that the electrical system functioned properly and reliably, supporting the car's overall performance.

3.3 Data Collection Techniques

This report draws on several data collection methods, as follows:

- Observation

Direct observation was used to collect the data needed for the study, such as cable resistance values measured with an avometer (multimeter). This method allowed data to be recorded in detail and with accuracy through direct observation.

- Testing

This study used a testing method based on measurements from a monitoring system adapted from Abdillah [6], designed to record data in real time and give an accurate picture of the parameters relevant to the study, especially those related to electrical energy consumption. This allowed the researchers to observe and analyze electricity-usage patterns in more detail and systematically. A central focus of this testing was

ISSN 3025-3780 (online)
ISSN 3025-4590 (printed)

measuring electricity consumption during the race, carried out with a joule meter, which precisely calculates the amount of electrical energy used over a given period. The results were then analyzed to assess the efficiency of energy use and to identify potential savings or further optimizations for similar situations in the future.

- Documentation

The documentation method is similar to direct observation, but the data collected takes the form of electronic documents (photographs) used to support and reinforce the research. This is consistent with documentation studies, a data-collection technique based on written and electronic documents [7].

- Data Analysis Technique

The data analysis technique used in this final project involved analyzing the electric current, voltage, and resistance measured in the circuit in order to determine the electric power used in the UG-22's electrical system. Data analysis techniques are the set of procedures used to process, interpret, and draw conclusions from data in a systematic way [6].

4. Result and Discussion

4.1 Design and Results of Electrical System Manufacturing

The electrical system design for the UG-22 in the Energy Efficient Car Competition had to prioritize efficiency, intelligent power management, and safety throughout its operation. It needed to be designed around the principles of energy efficiency, reliability, and safety. The design and its implementation in the car are shown in Fig. 3.

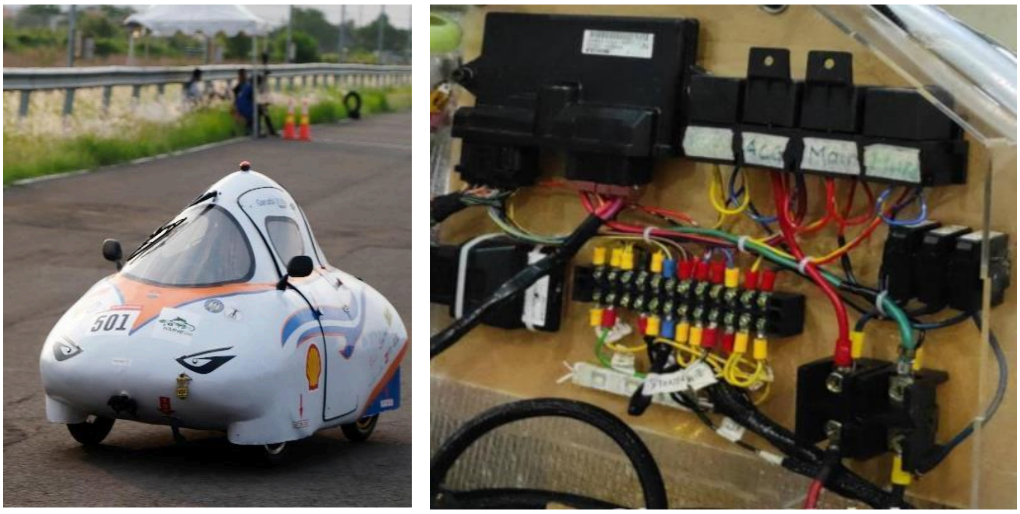

Fig.3 Implementation in the car

4.2 Analysis of Electrical System Results

Every electrical component has a significant effect on the car's electrical system and, in turn, on its energy consumption. In this case, the main problem with the electrical system was the high resistance found in the car during the previous year's competition. The researchers therefore sought to improve energy-consumption efficiency by reducing the resistance in the UG-22 car's electrical system.

Table 1. Electrical System Optimization Calculation

Condition	Cable / Material	Data Source	Voltage (V)	Voltage Drop (V)*	Resistance (Ω)	Energy Use (J)
Cable – before implementation	AVSS BF	2021 results	30	–	5.544×10^{4}	60
Cable – after deployment	AVSS	2022 results	30	–	5.412×10^{4}	30.3
Grounding – before application	–	2021 results	30	2.3	–	60
Grounding – after application	Silicone wire	2022 results	30	0.3	–	38.3

** Reported in the source data under the "Resistance" column heading for the grounding rows; retained here as originally presented.*

4.3 Optimization of the Electrical System Results

Reducing the resistance in the electrical system does not only improve electrical energy efficiency; it also has a positive effect on fuel consumption. With electrical energy used more efficiently, the UG-22 is better able to make use of its fuel, extending its range and improving its overall performance. This effect is especially valuable in competition, where every improvement in energy and fuel efficiency provides a competitive advantage. Optimizing the UG-22's electrical system therefore improves not only the car's technical performance but also its overall competitiveness.

Table 2. Calculation of Resistance Reduction

Parameter	Cable Length (m)	Resistance (Ω)	Energy Consumption (J)
Before implementation	92.4	5.544×10^4	60
After implementation	90.2	5.412×10^4	28.3
Reduction (impact)	2.2	1,320	21.7

4.4 Addition of the Grounding System

Adding a grounding system helps reduce resistance in the engine circuit. Resistance in the engine should be kept as low as possible, since it affects the responsiveness of the engine's sensors and, in turn, engine performance.

Table 3. Grounding Application Results

Parameter	Voltage Drop (V)	Energy Consumption (J)
Before implementation	3.3	60
After implementation	1.3	38.3
Reduction (impact)	2	31.78*

5. Conclusion

Based on the results and discussion presented above, this study concludes that resistance in the UG-22's electrical system can be reduced by replacing the cables with a lower-resistance type and by shortening the cable runs.

The voltage drop in the UG-22's electrical system can be reduced by adding a grounding system to the vehicle. Doing so reduced the voltage drop by 2 volts, which in turn reduced the amount of electrical energy consumed. Overall, optimizing the electrical system reduced the UG-22's electricity consumption from an initial 50 joules to 28.3 joules after optimization, a total reduction of 43.4%.

Author Contribution:

All authors contributed equally to the main contributor to this paper. All authors read and approved the final paper.

Funding:

This research received no external funding.

Acknowledgment:

The author would like to express gratitude to Universitas Negeri Yogyakarta for providing research facilities and support.

Conflicts of Interest:

The authors declare no conflict of interest.

References

[1] D. Linden and T. B. Reddy, Eds., Handbook of Batteries, 3rd ed. New York, NY, USA: McGraw-Hill, 2002.

[2] R. Afriwan, D. S. Putra, and Martias, "Pengaruh penggunaan voltage stabilizer terhadap konsumsi

ISSN 3025-3780 (online)
ISSN 3025-4590 (printed)

bahan bakar dan kandungan emisi gas buang pada sepeda motor Honda Vario 110 CC tahun 2009," Automotive Engineering Education Journals, vol. 6, no. 4, 2017.

[3] H. Abdi, B. Mohammadi-Ivatloo, S. Javadi, A. R. Khodaei, and E. Dehnavi, "Energy storage systems," in Distributed Generation Systems: Design, Operation and Grid Integration, G. B. Gharehpetian and S. M. Mousavi Agah, Eds. Oxford, U.K.: Butterworth-Heinemann, 2017, pp. 333–368, doi: 10.1016/B978-0-12-804208-3.00007-8.

[4] F. Ardiansyah, "Fungsi isolator pada kabel beserta bahan dan jenis isolator kabel," Pendidikan Elektronika, 2021.

[5] M. I. Fakhri and T. Sukarnoto, "Analisis chassis mobil hemat energi untuk Kontes KMHE tipe prototype Team HMM Usakti," Jurnal Penelitian dan Karya Ilmiah Lembaga Penelitian Universitas Trisakti, vol. 8, no. 2, pp. 330–336, 2023, doi: 10.25105/pdk.v8i2.15812.

[6] T. Ginting, "Pengaruh jenis busi terhadap konsumsi bahan bakar motor bakar 4 tak," Jurnal Informatika Kaputama (JIK), vol. 5, no. 1, pp. 89–98, 2021, doi: 10.59697/jik.v5i1.306.

[7] Nicolaus, G. S. Lubis, and M. Ivanto, "Studi pengaruh dan optimasi sistem transmisi pada kendaraan prototype kelas motor listrik Kontes Mobil Hemat Energi (KMHE) menggunakan metode Taguchi," JTRAIN: Jurnal Teknologi Rekayasa Teknik Mesin, vol. 5, no. 1, pp. 22–28, 2024.

[8] Balai Pengembangan Talenta Indonesia, Pedoman Kontes Mobil Hemat Energi Tahun 2023. Jakarta, Indonesia: Kementerian Pendidikan, Kebudayaan, Riset, dan Teknologi, 2023.

[9] J. V. Hutagaol, D. Setiawan, and H. Eteruddin, "Perancangan sistem monitoring kendaraan listrik," Jurnal Teknik, vol. 16, no. 1, pp. 96–102, 2022, doi: 10.31849/teknik.v16i1.9640.

JRAEE

Journal of Robotics, Automation, and Electronics Engineering
Vol. 3, No. 1, 2025, pp. 124-135
e-ISSN 3025-3780
https://journal.uny.ac.id/v3/jraee

Design of Pulse Induction Metal Detector for Metal Scanning in Food Integrated with Conveyor System

Isnanto Tris Gunawan[a,1], Moh. Khairudin[b,2,*]

[a, b]Dept. of Electrical and Electronic Engineering, Vocational Faculty, Universitas Negeri Yogyakarta
[1]isnantotris.2020@student.uny.ac.id; [2]moh_khairudin@uny.ac.id
[*]Corresponding Author

ARTICLE INFO

Article History
Received 22 Oct 2024
Revised 29 Aug 2026
Accepted 31 Aug 206

ABSTRACT

This research aims to develop a continuous metal detection system for food to prevent metal contamination in food consumed by the public and to determine the performance of a Programmable Logic Controller (PLC) system for controlling a metal detector conveyor. The method employed involves designing a PLC system that integrates a pulse induction metal detector, photosensor, and conveyor system. Functional testing is conducted on each component, followed by an overall performance test of the equipment. The functional testing results indicate that the components used can work properly and normally. The subsequent test is a performance test, which shows that out of 50 food samples tested, including meatballs, spring rolls, lumpia, cenil, and other traditional snacks, the device successfully detected metal in 25 of the food samples.

ABSTRAK

Penelitian ini bertujuan untuk membuat alat deteksi logam pada makanan secara kontinyu untuk mencegah kontaminasi logam pada makanan yang dikonsumsi masyarakat serta mengetahui unjuk kerja sistem Programmable Logic Controller (PLC) untuk kontrol alat konveyor detektor logam. Metode yang digunakan adalah rancang bangun sistem PLC yang mengintegrasikan detektor logam pulse induction, photosensor, dan sistem konveyor. Pengujian dilakukan secara fungsional pada masing-masing komponen dan uji kinerja alat secara keseluruhan. Hasil pengujian fungsional menunjukan bahwa komponen-komponen yang digunakan dapat bekerja dengan baik dan normal. Pengujian yang selanjutnya adalah pengujian kinerja yang menunjukan dari 50 sampel pengujian makanan seperti bakso, risol, lumpia, cenil dan jajanan pasar lainnya, alat berhasil mendeteksi 25 sampel makanan yang mengandung logam.

Keywords
Programmable Logic Controller;
Metal Detector;
Photosensor;
Conveyor;
Food

1. Introduction

In today's modern era, food quality is highly regarded in order to protect human health. Food safety is an important factor in national development and quality of life. In food processing, there is a risk of contamination by objects that can even be hazardous to health. One foreign object that is very dangerous when it enters food is metal, because when a person eats food containing foreign metal, the body, oral cavity, throat, and other parts of the digestive system can be injured. Therefore, it is important to apply metal detection devices in the food industry to prevent metal contamination in food. Rike Fitriani [1] and Steven Jendri Sokop [2] state that there are several reasons for developing a metal-separation device for food, namely the ease of transmitting data to a microcontroller for further development, low cost, flexibility, automatic control, and applicability from small to large scale.

Farhan Muhtarom [3] began with the development of a detection system capable of simultaneously identifying several types of metal. This identification can also make use of a conveyor belt, as in the studies by Livinti Petrua [4] and Catur Budi Waluyo [5]. Another study, by Gurit Pramudhito [6], was developed to create an intelligent algorithm for analyzing sensor data and identifying metal with high accuracy. In general, a metal detector works on the principle of generating a magnetic field through a transmitter coil and monitoring the signal induced in a receiver coil. A magnetic or electrically conductive object passing through the metal detector's magnetic field will alter the received signal, causing the receiver coil to detect the presence of a metal object in the food. To make detection run continuously, the metal detector is integrated with a belt conveyor system that is regulated and controlled using a microcontroller and a Programmable Logic Controller.

Based on prior research related to metal detectors in the food industry, which has been conducted extensively, the reason this study is important, and what distinguishes it from previous research, is the use of a metal detector system based on the pulse induction principle, integrated with a Programmable Logic Controller, thereby producing a system for sorting food that contains metal in the food industry.

2. Problem-Solving Approach

This chapter explains the supporting theory used in the process of designing and building a pulse induction metal detector for scanning metal in food integrated with a conveyor system. The basic theoretical review is tailored to the metal detector on the conveyor system so that it can serve as the methodological foundation for the research in the system design process.

2.1 Programmable Logic Controller

A PLC (Programmable Logic Controller) is a microcontroller-based device with input/output circuits that monitors the status of sensors connected on the input side and controls actuators installed as outputs according to the conditions desired by the user. A PLC has advantages over other computers in that it is protected against harsh operating conditions such as dust, humidity, and cold, and it provides extensive input/output configuration facilities [7].

One application of PLCs in industry is for the automation of conveyor systems. For a conveyor to operate automatically, an instrument and control system suited to the PLC and its programming must be designed. PLC studies and research are essentially dependent on the brand and type of PLC used [8].

2.2 Photosensor

A photosensor is a sensor that functions to detect the presence of an object, working by detecting infrared light or similar light emitted by a transmitter at a specific wavelength [9]. This sensor is often used in industry to provide an input signal or information for further control.

2.3 Metal Detector

Safety in food processing production is highly regarded by business operators in the food sector. This is because small pieces of metal contained in a food product can pose a safety hazard to the health of the consumer. The working principle of a metal detector uses the electromagnetic principle through a transmitter coil and monitors the signal induced by a receiver coil. Therefore, the use of metal detectors in the industrial sector is extensive, such as in the pharmaceutical, food, beverage, textile, and plastics industries, among others. There are several types of metal detectors, including:

2.3.1 VLF (Very Low Frequency) Metal Detector

As the name suggests, this detector uses a low-frequency signal to detect the presence of a metal object. The signal is transmitted through a wire coil, and when the signal approaches a metal object, the signal experiences a fluctuation that is then detected as the presence of metal.

2.3.2 Pulse Induction Metal Detector

This detector works with a high-voltage pulse to generate a magnetic field, which is then used to detect metal in an object. This detector is better at detecting metal at a greater distance compared to VLF.

Journal of Robotics, Automation, and Electronics Engineering
Vol. 3, No. 1, 2025, pp. 124-135
ISSN 3025-3780 (online)
ISSN 3025-4590 (printed)

2.3.3 BFO (Beat Frequency Oscillation) Metal Detector

This detector uses two oscillating coil sections to detect metal objects. One coil section generates a signal, and the other detects changes in the signal caused by the presence of metal around the coil.

2.3.4 MF (Multi-Frequency) Metal Detector

As the name suggests, this detector uses several frequencies to detect the presence of metal. This detector is more sensitive than a single-frequency detector. This signal is more stable than the signal of other detectors.

2.4 Buzzer

A buzzer consists of a coil mounted on a diaphragm; when the coil is supplied with electric current, it becomes an electromagnet, and the coil moves the diaphragm, thereby producing sound.

2.5 DC Motor

A DC motor is the main component of a variable-speed drive system. A DC motor requires a direct-voltage supply to its coil to convert it into mechanical energy. When a DC motor is supplied with direct voltage, a magnetic field is created in its stator coil [10]. This magnetic field attracts and repels the magnet on the rotor, causing the rotor to rotate. Therefore, DC motors are generally used in applications that require variable speed control, reliable speed regulation, and effective forward and reverse operation [11]. The DC motor in this study functions as the drive for the belt conveyor.

2.6 CX-Programmer Software

In today's modern era, control systems are one of the important areas of focus in industry. An effective and optimal control system is highly needed in industry today. A Programmable Logic Controller is a microprocessor used for industrial automation, such as control and monitoring. The language used in PLC programming is called ladder language, which consists only of input-process-output [12]. CX-Programmer was chosen as one of the software options for creating ladder language programs. Identification in the system takes the form of a High signal from the PLC, represented by the number 1 as an indicator that the I/O is active and the number 0 as an indicator that the I/O is inactive, according to the program.

3. Research Design

The research method used in the making of this final project is the Research and Development method. The stages and design concept of the metal-detection conveyor device in the final project titled “Design of a Pulse Induction Metal Detector for Metal Scanning in Food Integrated with a Conveyor System” are described in the form of a flowchart, as shown in Fig. 1, as follows:

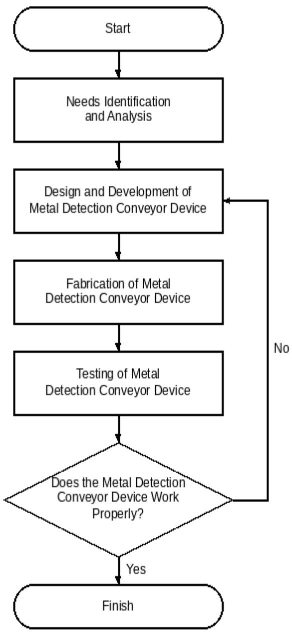

Fig.1 Flowchart of the research design stages and concept

3.1 Needs Identification and Analysis

Needs identification and analysis is the first stage in designing a metal-detection conveyor device. This stage is carried out to determine the conditions and problems in the field. The problems that have been identified are then analyzed to determine the solution to those problems.

3.1.1 Field Observation

Field observation was carried out at the Department of Electrical Engineering Education, Faculty of Engineering, UNY, and at CV Rumah Mesin. The observation was carried out by examining an example of how a PLC system works and how a food-sorting conveyor system works. Based on the observation results, the food-sorting system's quality control did not yet use a metal detector. As a result, food contaminated with metal could still occur, which could endanger the consumers of that food.

3.1.2 Needs Analysis

Based on the observation results, it is known that maintaining food quality is important for food producers. This is done to protect the safety of food consumers so that they avoid ingesting metal objects. Therefore, a metal-detector device that can operate continuously is needed to sort food after production, making the process more effective and efficient.

3.1.3 Solution Search

Based on the needs analysis carried out, the solution provided to address the need for a metal detector that can operate continuously, effectively, and efficiently is to build a PLC system on the conveyor that combines a metal detector, a photosensor, and the conveyor system itself.

3.2 Device Planning

This stage is intended to produce the design and planning of the device that will later serve as a reference in the device development process. In addition, the device-planning stage is intended to reduce the possibility of errors in the device development process while also ensuring that the device can operate as expected. This device-planning stage covers the design of the hardware and software. The device-planning process in this final project is as follows:

3.2.1 Device Workflow

The first stage in the device-planning process is designing the device's workflow. The design process for the device's workflow is carried out by creating a flowchart and a system block diagram. The system flowchart for the PLC-based metal detector system for food is shown in Fig. 2, as follows:

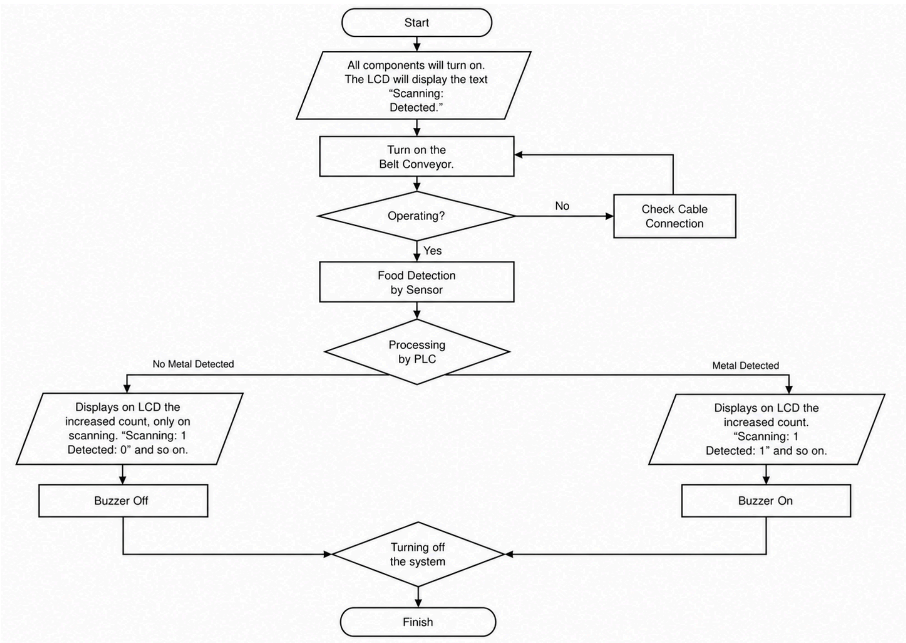

Fig.2 Flowchart system

The operational process of the metal-detection device for food begins by connecting the single-phase power source, activating the miniature circuit breaker (MCB), and turning on the power supply for the metal-detector module. Next, the belt conveyor is operated by pressing the Start/ON button on the control panel. Food is placed on the operating belt conveyor. The first sensor detects the presence of food, and the dual metal sensor identifies metal contamination in the food. When food is detected to contain metal, a signal is sent to the Programmable Logic Controller (PLC), which activates the warning buzzer. The Liquid Crystal Display (LCD) displays the number of food items scanned and detected as containing metal. The system can be turned off by pressing the Stop/OFF button, disconnecting the MCB, turning off the power supply, and unplugging the cable from the power source.

A system block diagram was also created to represent the relationship between one component and another in the system, in the form of interconnected blocks, as shown in Fig. 3, as follows:

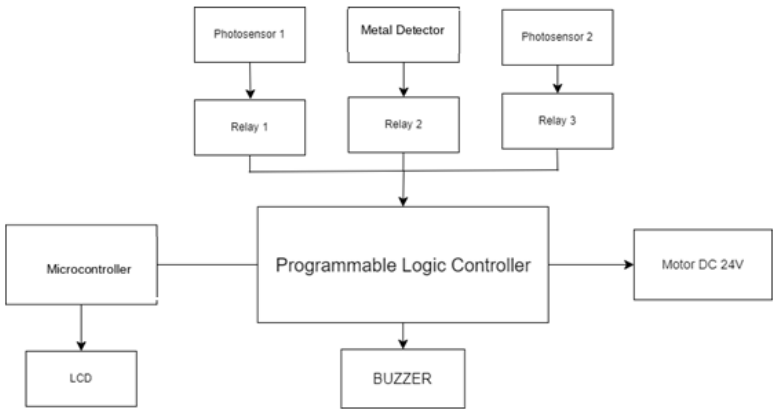

Fig.3 Block diagram

3.2.2 Hardware Design

The second stage of the device design and design process is designing the hardware. This stage involves electrical design. The electrical design stage aims to design the pin or terminal connections between one component and another so as to create a unified device that can operate. This electrical design is shown in Fig. 4, as follows:

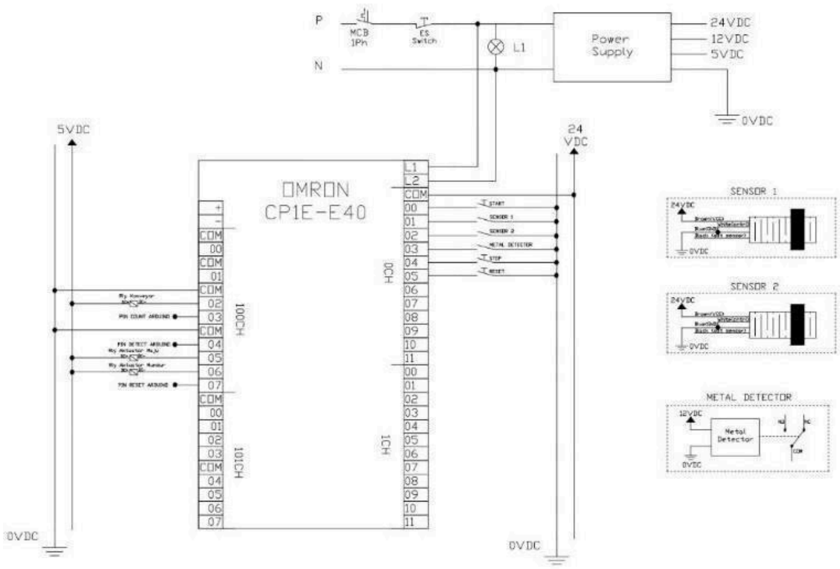

Fig.4 PLC wiring design

3.2.3 Software Design

The second stage of device design is designing the software. This stage covers the series of processes for creating the software for the metal-detection system for food integrated with the conveyor system. This software design stage uses CX-Programmer and Arduino IDE software. The program created using Arduino

IDE is shown in the program code below:

```
#include <Arduino.h>
#include <LiquidCrystalIO.h>
#include <IoAbstractionWire.h>
#include <Wire.h>
#define counter A0
#define deteksi A1
#define vcc 13

int hasil01, hasil02, pb1=0, pb2=0;
//LiquidCrystal_I2C lcd(0x27,16,2);
LiquidCrystalI2C_RS_EN(lcd, 0x27, false)

void setup()
{
 //lcd.begin();
 Wire.begin();
 lcd.begin(16, 2);
 lcd.configureBacklightPin(3);
 lcd.backlight();

 pinMode(counter, INPUT);
 pinMode(deteksi, INPUT);
 pinMode(vcc, OUTPUT);
}

void loop()
{
 int cnt=digitalRead(counter);
 int det=digitalRead(deteksi);
 digitalWrite(vcc, HIGH);

 if(cnt==HIGH){pb1=1;}
 if(cnt==LOW && pb1==1)
 {hasil01++; pb1=0;}
 if(det==HIGH){pb2=1;}
 if(det==LOW && pb2==1)
 {hasil02++; pb2=0;}

 lcd.setCursor(0,0);
 lcd.print("Scanning =");
 lcd.setCursor(0,1);
 lcd.print("Terdeteksi=");
 lcd.setCursor(12,0);
 lcd.print(hasil01);
 lcd.setCursor(12,1);
 lcd.print(hasil02);
}
```

The PLC program created using CX-Programmer is shown in Fig. 5 below:

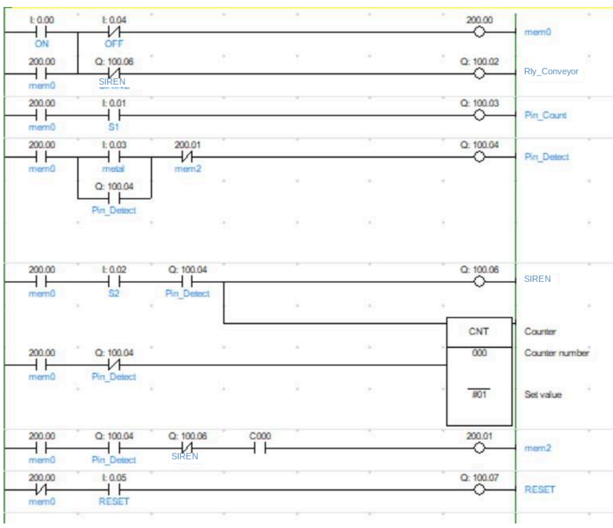

ISSN 3025-3780 (online)
ISSN 3025-4590 (printed)

Fig. 5 PLC Program using CX-Programmer software

4. Research Results

This chapter discusses the results of the research that has been conducted, as well as the test results of the device that has been built.

4.1 Hardware Fabrication Results

The fabrication of the hardware in this final project involves building and installing the components and wiring according to the planning design. The results of this hardware fabrication can be seen in Fig. 6 and Fig. 7, as follows:

Fig. 6 Installation of electrical components

Fig.7 Metal detector conveyor device

4.2 Test Results

The first test conducted was the functional test of the device. This test was carried out by testing all the electronic components in the system with the aim of ensuring that each component in the system can function and operate according to the plan.

The second test was the performance test of the device. This test was carried out with the aim of testing and ensuring that the entire metal-detector conveyor device can operate properly, reliably, and accurately in detecting metal in food. The results of the final project testing are as follows:

4.2.1 Functional Test

The functional test in this final project aims to ensure the function and accuracy of each component used.

The test results then become considerations for whether the component is suitable for use. The following are the test results for each component tested:

Table 1. Functional Test Results of Photosensor 1

No	Food Name	Test Result (Distance 0–25 cm)
1	Meatballs	Detected
2	Nugget	Detected
3	Lemper	Detected
4	Arem-arem	Detected
5	Spring Rolls	Detected
6	Fried Snacks	Detected
7	Lumpia	Detected
8	Martabak	Detected
9	Steamed Cake	Detected
10	Boiled Egg	Detected

Table 2. Functional Test Results of Photosensor 2

No	Food Name	Test Result (Distance 0–25 cm)
1	Meatballs	Detected
2	Nugget	Detected
3	Lemper	Detected
4	Arem-arem	Detected
5	Spring Rolls	Detected
6	Fried Snacks	Detected
7	Lumpia	Detected
8	Martabak	Detected
9	Steamed Cake	Detected
10	Boiled Egg	Detected

Table 3. Metal Detector Test Results

No	Food Name	Staple Metal Present	Metal Detector Result
1	Meatballs	Present	Detected
2	Nugget	Absent	Not Detected
3	Lemper	Present	Detected
4	Arem-arem	Absent	Not Detected
5	Spring Rolls	Present	Detected
6	Fried Snacks	Absent	Not Detected
7	Lumpia	Present	Detected
8	Martabak	Absent	Not Detected
9	Steamed Cake	Present	Detected
10	Boiled Egg	Absent	Not Detected

Table 4. PLC Input Pin Test Results

No	Output Signal (Program)	Input PIN	Result
1	-	L1	Normal
2	-	L2	Normal
3	-	COM	Normal
4	0	00 – 11 (0CH)	0
5	1	00 (0CH)	1
6	1	01 (0CH)	1
7	1	02 (0CH)	1
8	1	03 (0CH)	1
9	1	04 (0CH)	1
10	1	05 (0CH)	1
11	1	06 (0CH)	1
12	1	07 (0CH)	1
13	1	08 (0CH)	1
14	1	09 (0CH)	1
15	1	10 (0CH)	1
16	1	11 (0CH)	1
17	0	00 – 11 (1CH)	0
18	1	00 (1CH)	1
19	1	01 (1CH)	1
20	1	02 (1CH)	1
21	1	03 (1CH)	1
22	1	04 (1CH)	1
23	1	05 (1CH)	1

24	1	06 (1CH)	1
25	1	07 (1CH)	1
26	1	08 (1CH)	1
27	1	09 (1CH)	1
28	1	10 (1CH)	1
29	1	11 (1CH)	1

Table 5. PLC Output Pin Test Results

No	Output Signal (Program)	Output PIN	Result
1.	-	+	Normal
2.	-	-	Normal
3.	-	COM (100CH)	Normal
4.	-	COM (100CH)	Normal
5.	-	COM (100CH)	Normal
6.	-	COM (100CH)	Normal
7.	0	00 – 07 (100CH)	0
8.	1	00 (100CH)	1
9.	1	01 (100CH)	1
10.	1	02 (100CH)	1
11.	1	03 (100CH)	1
12.	1	04 (100CH)	1
13.	1	05 (100CH)	1
14.	1	06 (100CH)	1
15.	1	07 (100CH)	1
16.	-	COM (101CH)	Normal
17.	-	COM (101CH)	Normal
18.	0	00 – 07 (101CH)	0
19.	1	00 (101CH)	1
20.	1	01 (101CH)	1
21.	1	02 (101CH)	1
22.	1	03 (101CH)	1
23.	1	04 (101CH)	1
24.	1	05 (101CH)	1
25.	1	06 (101CH)	1
26.	1	07 (101CH)	1

Table 6. Relay 1 Test Results

No	Input Voltage (Volt)	Initial Relay Condition	Final Relay Condition
1	5	NC	NO
2	0	NO	NC

Table 7. Relay 2 Test Results

No	Input Voltage (Volt)	Initial Relay Condition	Final Relay Condition
1	5	NC	NO
2	0	NO	NC

Table 8. Relay 3 Test Results

No	Input Voltage (Volt)	Initial Relay Condition	Final Relay Condition
1	5	NC	NO
2	0	NO	NC

Table 9. Push Button Test Results

No	Push Button Condition	Active	Inactive
1	Normal / Not Pressed	x	✓
2	Pressed Once	✓	x

Table 10. Buzzer Test Results

No	Input Voltage (Volt)	Buzzer Condition
1	12	Active
2	0	Inactive

Based on the functional testing conducted, it can be determined that the electronic components used can run or operate normally and accurately. This functional testing also serves to ensure that the electronic components used in this final project can be properly integrated and produce a device that can operate normally as planned.

4.2.2 Performance Test

The performance test in this final project aims to determine the overall function of the system in this metal-detector conveyor. The performance test in this final project was carried out 50 times using various types of food. Meanwhile, 25 of the 50 food types used for the performance test contained staple metal. The testing process was carried out by monitoring the sensors, buzzer, and LCD. The results of the performance test in this final project can be seen in Table 11 below:

Table 11. Performance Test Results

No	Food Variation	Contains Metal (Staples)	Photosensor 1	Metal Detector	Photosensor 2	Buzzer	Scanning	Detected
1	Meatballs	Present	Detected	Detected	Detected	Active	1	1
2	Martabak	Absent	Not Detected	Not Detected	Not Detected	Inactive	2	1
3	Fried Snacks	Absent	Not Detected	Not Detected	Not Detected	Inactive	3	1
4	Soto	Absent	Not Detected	Not Detected	Not Detected	Inactive	4	1
5	Carabikang	Absent	Not Detected	Not Detected	Not Detected	Inactive	5	1
6	Spring Rolls	Present	Detected	Detected	Detected	Active	6	2
7	Lontong	Present	Detected	Detected	Detected	Active	7	3
8	Nasi Kucing	Absent	Not Detected	Not Detected	Not Detected	Inactive	8	3
9	Lemper	Absent	Not Detected	Not Detected	Not Detected	Inactive	9	3
10	Fried Tofu	Present	Detected	Detected	Detected	Active	10	4
11	Kue Ku	Present	Detected	Detected	Detected	Active	11	5
12	Serabi	Present	Detected	Detected	Detected	Active	12	6
13	Empek-empek	Present	Detected	Detected	Detected	Active	13	7
14	Fried Noodles	Absent	Not Detected	Not Detected	Not Detected	Inactive	14	7
15	Pastel	Absent	Not Detected	Not Detected	Not Detected	Inactive	15	7
16	Toasted Bread	Absent	Not Detected	Not Detected	Not Detected	Inactive	16	7
17	Tiwul	Absent	Not Detected	Not Detected	Not Detected	Inactive	17	7
18	Yangko	Absent	Not Detected	Not Detected	Not Detected	Inactive	18	7
19	Dadar Gulung	Present	Detected	Detected	Detected	Active	19	8
20	Otak-otak	Absent	Not Detected	Not Detected	Not Detected	Inactive	20	8
21	Bakwan	Present	Detected	Detected	Detected	Active	21	9
22	Cilok	Absent	Not Detected	Not Detected	Not Detected	Inactive	22	9
23	Satay	Present	Detected	Detected	Detected	Active	23	10
24	Combro	Absent	Not Detected	Not Detected	Not Detected	Inactive	24	10
25	Kue Lumpur	Present	Detected	Detected	Detected	Active	25	11
26	Getuk	Absent	Not Detected	Not Detected	Not Detected	Inactive	26	11
27	Nagasari	Absent	Not Detected	Not Detected	Not Detected	Inactive	27	11
28	Putu	Absent	Not Detected	Not Detected	Not Detected	Inactive	28	11
29	Kue Talam	Present	Detected	Detected	Detected	Active	29	12
30	Bolu Kukus	Present	Detected	Detected	Detected	Active	30	13
31	Monte	Absent	Not Detected	Not Detected	Not Detected	Inactive	31	13
32	Terang Bulan	Absent	Not Detected	Not Detected	Not Detected	Inactive	32	13
33	Kue Pancong	Absent	Not Detected	Not Detected	Not Detected	Inactive	33	13
34	Kue Mangkok	Present	Detected	Detected	Detected	Active	34	14
35	Pukis	Present	Detected	Detected	Detected	Active	35	15
36	Cireng	Absent	Not Detected	Not Detected	Not Detected	Inactive	36	15
37	Wingko Babat	Present	Detected	Detected	Detected	Active	37	16
38	Kue Cubit	Absent	Not Detected	Not Detected	Not Detected	Inactive	38	16

ISSN 3025-3780 (online)
ISSN 3025-4590 (printed)

39	Jenang	Present	Detected	Detected	Detected	Active	39	17
40	Lapis Legit	Absent	Not Detected	Not Detected	Not Detected	Inactive	40	17
41	Crackers	Present	Detected	Detected	Detected	Active	41	18
42	Kue Sus	Absent	Not Detected	Not Detected	Not Detected	Inactive	42	18
43	Gemblong	Present	Detected	Detected	Detected	Active	43	19
44	Kue Rangi	Present	Detected	Detected	Detected	Active	44	20
45	Klepon	Present	Detected	Detected	Detected	Active	45	21
46	Kue Mangkok	Absent	Not Detected	Not Detected	Not Detected	Inactive	46	21
47	Onde-onde	Present	Detected	Detected	Detected	Active	47	22
48	Kue Cucur	Present	Detected	Detected	Detected	Active	48	23
49	Lupis	Present	Detected	Detected	Detected	Active	49	24
50	Kue Cenil	Present	Detected	Detected	Detected	Active	50	25

The test results shown in Table 11 indicate that the overall system works normally and accurately because, when the food contains metal, the metal detector detects it, and the photosensors also detect the presence of food passing along the belt conveyor. When the metal detector detects metal in the food, the food then passes the second photosensor, which causes the buzzer to turn on, serving as an indicator to the operator that the food contains metal. The LCD also displays the scanning and detected count according to the data.

5. Conclusion

Based on the results of the testing and discussion in this final project on the design and construction of a pulse induction metal detector for scanning metal in food integrated with a conveyor system, the conclusions are as followings

The development of this final project on the design and construction of a pulse induction metal detector for scanning metal in food integrated with a conveyor system began with needs identification and analysis. The components required in the development of this final project are a conveyor, an Omron CP1E-E40 PLC, relays, a photosensor, a pulse induction metal detector, a buzzer, an Arduino Uno, an LCD, and a power supply. After determining the system requirements, the next process is the design and planning of the device, device development, and device testing until the PLC system for scanning food with the photosensor and PI metal detector integrated with the conveyor system can operate properly, reliably, and accurately according to the initial plan.

The first stage of testing was the functional test. The results of the functional test on the pulse induction metal detector system for scanning metal in food integrated with a conveyor system show that each component used can function normally. The test results for the three main sensors, namely the two photosensors and one metal detector, show that these sensors work accurately.

The performance test results show that the system can work according to the plan, namely being able to detect metal contained in food. The test was carried out with 50 trials using various types of traditional market snacks, such as meatballs, martabak, fried snacks, klepon, etc. The test was carried out at least 50 times to ensure that the device built can work normally, reliably, and accurately. The performance test results show that photosensor 1, photosensor 2, the metal detector, the Arduino Uno, the LCD, and the buzzer can be properly integrated and work well.

Author Contribution:

All authors contributed equally to the main contributor to this paper. All authors read and approved the final paper.

Funding:

This research received no external funding.

Acknowledgment:

The author would like to express gratitude to Universitas Negeri Yogyakarta for providing research facilities and support.

Conflicts of Interest:

The authors declare no conflict of interest.

References

[1] R. Fitriani and N. Paramytha, "Robot pendeteksi logam dengan mikrokontroler," in Bina Darma Conference on Engineering Science (BDCES), vol. 2, no. 1, pp. 165–173, 2020. Metadata penulis, volume, nomor, dan halaman ini juga tercantum dalam daftar rujukan artikel terkait di ORBITH.

[2] S. J. Sokop, D. J. Mamahit, and S. R. U. A. Sompie, "Trainer periferal antarmuka berbasis mikrokontroler Arduino Uno," Jurnal Teknik Elektro dan Komputer, vol. 5, no. 3, pp. 13–23, 2016, doi: 10.35793/jtek.v5i3.11999.

[3] F. Muhtarom and H. Effendi, "Alat pendeteksi logam pada makanan berbasis Arduino Uno," JTEIN: Jurnal Teknik Elektro Indonesia, vol. 1, no. 2, pp. 43–48, 2020, doi: 10.24036/jtein.v1i2.14.

[4] P. Livinti and M. Ghandour, "PWM control of a DC motor used to drive a conveyor belt," Procedia Engineering, vol. 100, pp. 299–304, 2015, doi: 10.1016/j.proeng.2015.01.371.

[5] C. B. Waluyo, A. F. Maksum, and P. Setiawan, "Rancang bangun alat pemilah makanan mengandung logam berbasis Arduino," ORBITH: Majalah Ilmiah Pengembangan Rekayasa dan Sosial, vol. 19, no. 3, pp. 273–279, 2023, doi: 10.32497/orbith.v19i3.5259.

[6] G. Pramudhito, "Prototipe conveyor belt penyortir objek berdasarkan warna menggunakan kamera Pixy2 dan Arduino ATmega328 dengan aplikasi Visual Basic," undergraduate thesis, Universitas Diponegoro, Semarang, Indonesia, 2021.

[7] S. Chitra and V. Raghavan, "Conveyor control using programmable logic controller," International Journal of Advancements in Research & Technology, vol. 3, no. 8, pp. 25–31, 2014.

[8] Z. F. Ikatrinasari, H. Herlambang, and K. Kosasih, "Design and implementation of intelligent electronic component inspection based on PLC and vision system," Jurnal Sistem dan Manajemen Industri, vol. 7, no. 2, pp. 155–168, 2023, doi: 10.30656/jsmi.v7i2.6511.

[9] G. M. Gu, Y. K. Shin, J. Son, and J. Kim, "Design and characterization of a photo-sensor based force measurement unit (FMU)," Sensors and Actuators A: Physical, vol. 182, pp. 49–56, 2012, doi: 10.1016/j.sna.2012.05.018.

[10] Y. Cheng, X. Lyu, and S. Mao, "Optimization design of brushless DC motor based on improved JAYA algorithm," Scientific Reports, vol. 14, Art. no. 5427, 2024, doi: 10.1038/s41598-024-54582-z.

[11] R. A. Ahmed and E. D. Hassan, "Modeling, design and control of speed DC motor using chopper," International Journal of Electrical and Electronics Research (IJEER), vol. 11, no. 4, pp. 1162–1166, 2023, doi: 10.37391/ijeer.110437.

[12] B. Setiawan, "Rancang bangun sistem simulasi pemasangan tutup botol berdasarkan warna terkendali PLC," unpublished manuscript, Universitas Sebelas Maret, Surakarta, Indonesia, 2022. [Online]. Available: ResearchGate.

JRAEE

Journal of Robotics, Automation, and Electronics Engineering
Vol. 3, No. 1, 2025, pp. 143-152
e-ISSN 3025-3780
https://journal.uny.ac.id/v3/jraee

Design and Performance Evaluation of a Programmable Logic Controller-Based Water Treatment Automation System

Muhammad David Adha Wardana[a,1], Rohjai Badarudin[b,2,*]

[a, b]Dept. of Electrical and Electronics Engineering, Vocational Faculty, Universitas Negeri Yogyakarta
[1]muhammaddavid.2020@student.uny.ac.id; [2]rohjai.badarudin@uny.ac.id
[*]Corresponding Author

ARTICLE INFO

Article History
Received 28 Oct 2024
Revised 29 Aug 2026
Accepted 31 Aug 2026

Keywords
Programmable Logic Controller;
SCADA;
Water Treatment Automation;
Human-Machine Interface;
Chlorine Dosing.

ABSTRACT

Small-scale water-treatment units often rely on manually sequenced pumps, mixers, and chemical dosing, which can cause inconsistent operation and limited process visibility. This study develops and evaluates a laboratory-scale automation system based on an Omron CP1H-XA40DR-A programmable logic controller (PLC) integrated with a Wonderware InTouch supervisory control and data acquisition (SCADA) interface. The main contribution is a low-complexity PLC-SCADA architecture that combines one-button sequential operation with quantitative evaluation of functional logic, HMI response, batch-volume repeatability, and chlorine-dose screening. The system was developed through requirement analysis, electrical and mechanical design, ladder-program implementation, SCADA visualization, fabrication, and experimental testing. Functional testing covered six command-state combinations, HMI response time was measured for seven components, and ten filling cycles were analyzed for water-height and volume consistency. Calcium hypochlorite was screened at calculated masses of 4.44 mg and 13.33 mg for 2 L batches. All six control-state tests were successful. Mean HMI response time was 0.543 ± 0.282 s (0.2-1.0 s). Mean water height and volume were 10.72 ± 0.13 cm and 2.236 ± 0.027 L, with coefficients of variation of 1.23% and 1.22%. At 4.44 mg, all ten samples were reported colorless and without detectable odor or taste; at 13.33 mg, slight chlorine odor and slight bitter taste were each reported in five samples. The prototype demonstrates reliable sequential control and repeatable laboratory-scale filling; however, the water-quality results are only organoleptic screening because residual chlorine, turbidity, pH, and microbiological safety were not measured.

ABSTRAK

Unit pengolahan air skala kecil masih sering mengandalkan pengoperasian pompa, pengaduk, dan penambahan bahan kimia secara manual sehingga berpotensi menimbulkan ketidakkonsistenan proses dan keterbatasan pemantauan. Penelitian ini mengembangkan dan mengevaluasi sistem otomasi skala laboratorium berbasis programmable logic controller (PLC) Omron CP1H-XA40DR-A yang terintegrasi dengan supervisory

Journal of Robotics, Automation, and Electronics Engineering
Vol. 3, No. 1, 2025, pp. 143-151
ISSN 3025-3780 (online)
ISSN 3025-4590 (printed)

control and data acquisition (SCADA) Wonderware InTouch. Kontribusi utama penelitian adalah arsitektur PLC-SCADA ber kompleksitas rendah yang menggabungkan operasi berurutan dengan satu tombol dan evaluasi kuantitatif terhadap logika fungsi, respon HMI, keterulangan volume batch, serta skrining dosis kaporit. Sistem dikembangkan melalui analisis kebutuhan, perancangan elektrikal dan mekanikal, implementasi ladder diagram, visualisasi SCADA, fabrikasi, dan pengujian eksperimental. Pengujian fungsi mencakup enam kombinasi perintah-kondisi, waktu respons HMI diukur pada tujuh komponen, dan sepuluh siklus pengisian dianalisis untuk menilai konsistensi tinggi serta volume air. Kalsium hipoklorit diuji pada masa terhitung 4,44 mg dan 13,33 mg untuk batch 2 L. Seluruh enam pengujian logika kendali berhasil. Rata-rata waktu response HMI adalah 0,543 ± 0,282 s (0,2-1,0 s). Tinggi dan volume air rata-rata masing-masing 10,72 ± 0,13 cm dan 2,236 ± 0,027 L, dengan koefisien variasi 1,23% dan 1,22%. Pada dosis 4,44 mg, seluruh sepuluh sampel dilaporkan tidak berwarna serta tanpa bau atau rasa yang terdeteksi; pada 13,33 mg, sedikit bau kaporit dan sedikit rasa pahit masing-masing muncul pada lima sampel. Prototipe menunjukkan kendali berurutan yang andal dan pengisian yang konsisten pada skala laboratorium, tetapi hasil kualitas air hanya merupakan skrining organoleptik karena residu klorin, kekeruhan, pH, dan keamanan mikrobiologis belum diukur.

1. Introduction

Water treatment plants increasingly combine programmable control, supervisory visualization, and online sensing to reduce manual intervention and improve process consistency. PLC-SCADA architectures remain attractive because they provide deterministic sequencing, straightforward integration with pumps and relays, and operator-oriented monitoring [1]. At the same time, recent reviews of water and wastewater treatment automation emphasize the growing role of real-time monitoring, advanced process control, and digital data infrastructures in improving operational reliability and resource efficiency [2], [3]. Recent implementations have also shown that PLC-based monitoring can be coupled with IoT or long-range communication to extend data access and water-quality supervision beyond local control panels [4], [5].

The state of the art is moving from conventional supervisory systems toward digital twins, model updating, anomaly detection, and data-driven optimization. Microservice-based digital-twin platforms have been proposed to integrate process models, real-time data, and maintenance information [6], while full-scale operational digital twins have demonstrated the value of automated data pipelines and operator interfaces for treatment facilities [7]. Real-time data-processing and anomaly-detection frameworks further show how plant data can support continuous model adaptation and fault awareness [8], [9]. More recent work has extended this direction toward machine-learning-enabled digital twins for proactive process control and maintenance [10]. These approaches are powerful, but they typically require richer instrumentation, larger datasets, and more complex computing infrastructure than is available in many laboratory-scale, educational, or small treatment systems.

At the process-control level, current research increasingly addresses online management, reinforcement-learning optimization, sensor-driven control, and intelligent chemical dosing [11]-[14]. For drinking-water treatment, data-driven coagulant dosing models have been developed using dissolved-organic-carbon signals, graph-attention time-series models, and large-scale deep learning datasets [15]-[17]. Chlorine management also requires careful monitoring because the relationship between the applied dose and the residual disinfectant depends on water characteristics, contact time, and system dynamics [18], [19]. Advanced economic model-predictive control has additionally demonstrated the potential of learned process models to improve treatment operation [20]. Nevertheless, a robust low-complexity automation baseline remains relevant when the primary engineering objective is to replace manual sequencing, ensure repeatable batch operation, and provide clear supervisory feedback before more advanced closed-loop control is introduced.

This study therefore develops and experimentally evaluates a laboratory-scale PLC-based water-treatment automation system using an Omron CP1H-XA40DR-A and Wonderware InTouch. The contribution of the research is fourfold: (1) an integrated one-button sequential control architecture for filling, chemical addition, mixing, and transfer; (2) quantitative verification of command-state logic and HMI response time; (3) repeatability analysis of water height and batch volume over repeated cycles; and (4) a more cautious interpretation of calcium hypochlorite dosing based on the available organoleptic observations. In contrast with studies that focus on high-level optimization, the present work establishes and evaluates the reliability of the basic automation layer that can later be extended with level, flow, pH, turbidity, and residual-chlorine feedback.

2. Method

2.1 System Architecture and Operating Sequence

The prototype was developed using an engineering design-build-test workflow consisting of requirements identification, electrical and mechanical design, PLC programming, SCADA configuration, prototype fabrication, and functional testing. The main controller is an Omron CP1H-XA40DR-A PLC. The actuator layer consists of three water pumps and one mixing motor driven through relays, while three push buttons provide START, OFF, and STOP commands. A 24 V power supply and terminal distribution are used for the control circuit. Wonderware InTouch is used as a virtual human-machine interface (HMI) to visualize the active process state.

The process begins when the START command is accepted by the PLC. Pump 1 transfers source water to the treatment vessel. After the programmed filling interval, Pump 1 is deactivated and Pump 2 adds the prepared calcium hypochlorite solution. The mixer is then activated for the programmed mixing interval. Finally, Pump 3 transfers the treated batch to the downstream container. The HMI indicates the active pump, mixer, and command-lamp states throughout the sequence. The STOP command interrupts operation temporarily, whereas OFF terminates operation according to the implemented logic.

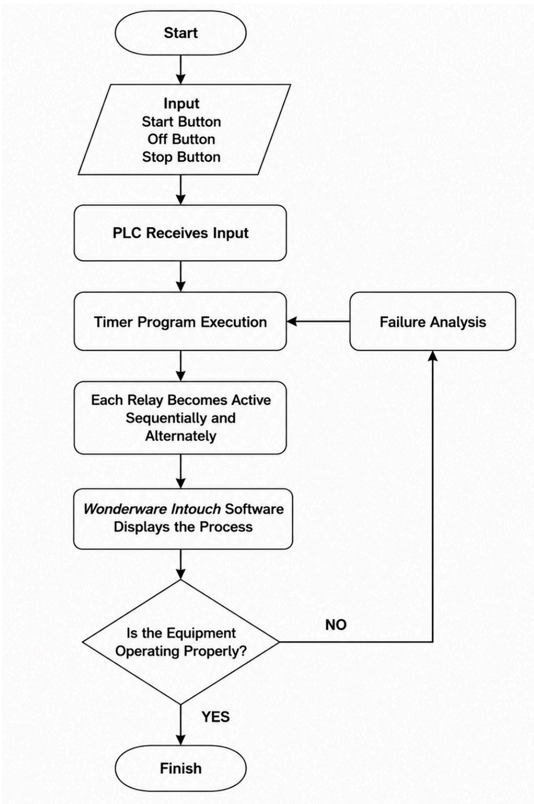

Fig. 1 Operational flow of the PLC-based water-treatment sequence

ISSN 3025-3780 (online)
ISSN 3025-4590 (printed)

2.2 Hardware and Software Implementation

The electrical design separates low-voltage control signals from the actuator switching path through relay interfaces. The PLC receives push-button inputs and energizes relay outputs corresponding to Pump 1, Pump 2, the mixer motor, and Pump 3. The mechanical prototype uses a rack-type frame to hold the PLC, power supply, control panel, treatment vessel, chemical container, pumps, mixer, and display equipment. The dimensions and component arrangement follow the original prototype design and were retained without modification in this revised manuscript.

The PLC program was created in CX-Programmer using ladder logic and timer-based sequencing. Wonderware InTouch was configured as the supervisory layer. The HMI mirrors the operating state of the actuators and command indicators, allowing the operator to verify whether the physical process and displayed state are synchronized. In this prototype, the sequence is primarily timer based; therefore, it should be regarded as an open-loop batch automation architecture rather than a closed-loop water-quality control system.

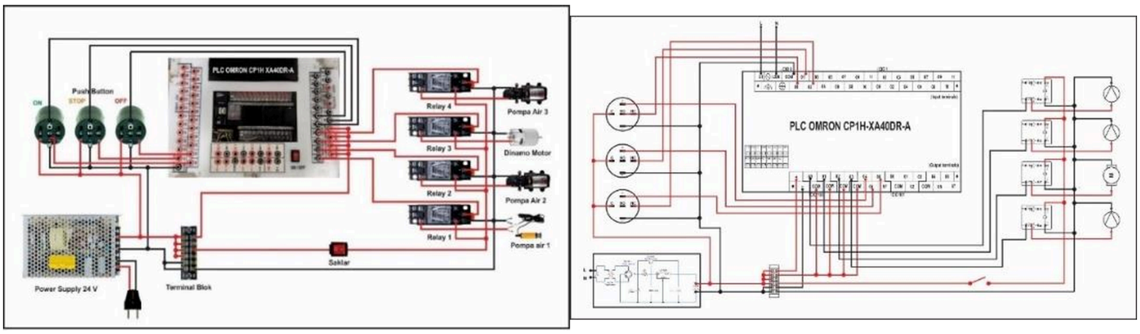

(a) Component wiring (b) Wiring diagram

Fig. 2 Electrical design: (a) component wiring and (b) wiring diagram

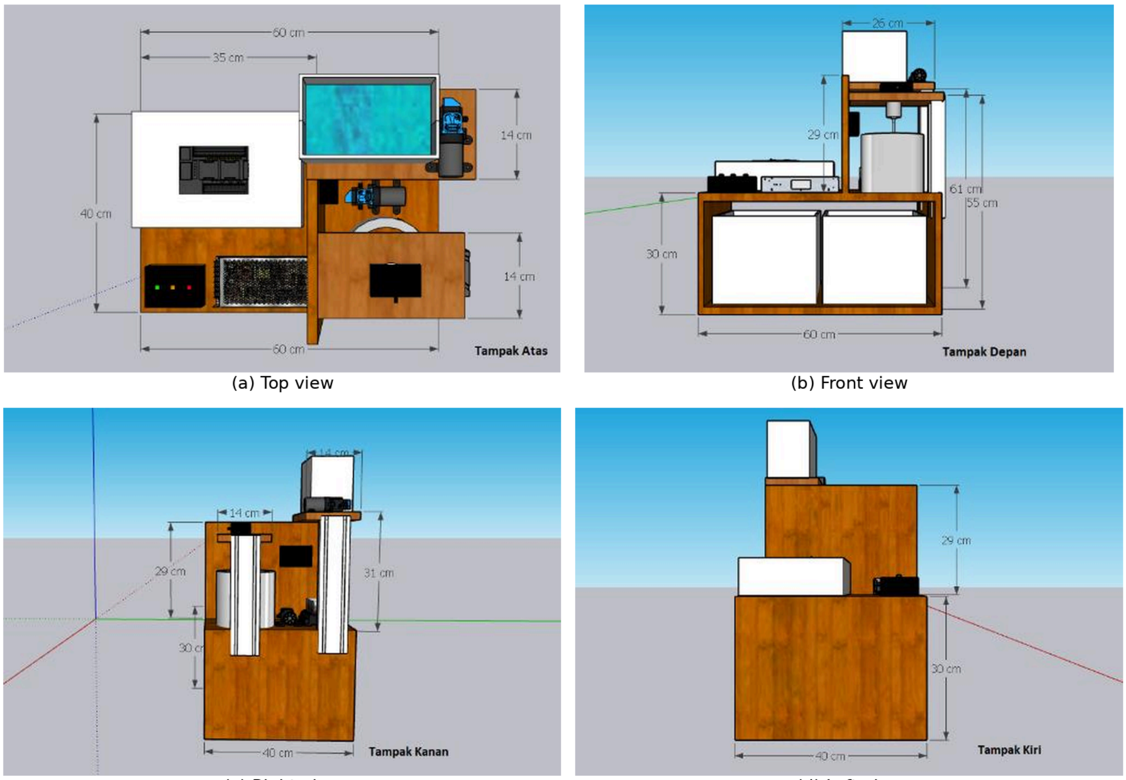

(a) Top view (b) Front view

(c) Right view (d) Left view

Fig. 3 Mechanical design of the laboratory-scale prototype

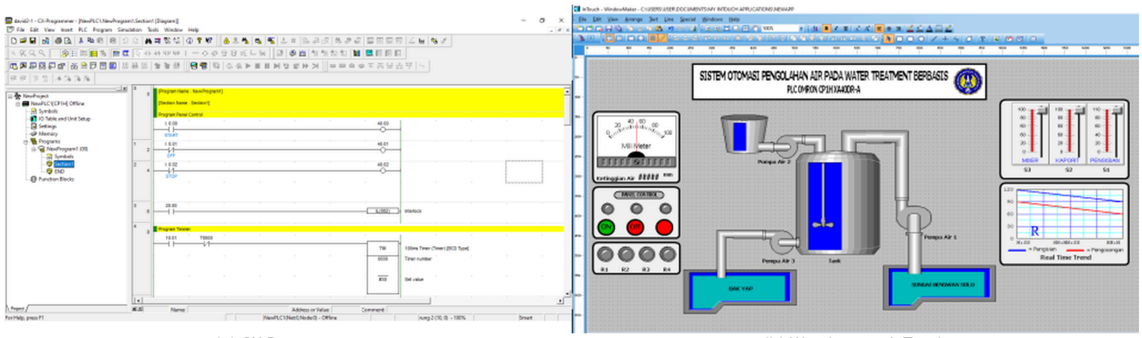

(a) CX-Programmer (b) Wonderware InTouch

Fig. 4 Software environment used for PLC programming and SCADA visualization

2.3 Experimental Evaluation

Four evaluations were performed using the measurements reported in the original experiment. First, functional state-transition testing examined six combinations of command input and initial system state to verify ON, OFF, and STOP behavior. Second, HMI response time was recorded for seven monitored components: three pumps, the mixer, and the START, OFF, and STOP indicator lamps. Third, filling repeatability was evaluated over ten cycles using the recorded water height and calculated batch volume. Fourth, the effect of two nominal calcium hypochlorite doses was screened from the reported color, odor, and taste observations over ten repetitions per dose.

For chlorine preparation, the required calcium hypochlorite mass was calculated as $m = (C \times V)/f$, where m is the calcium hypochlorite mass, C is the nominal chlorine dose, V is the water volume, and f is the available-chlorine fraction. Using $V = 2$ L and $f = 0.90$, nominal doses of 2 mg/L and 6 mg/L correspond to 4.44 mg and 13.33 mg of calcium hypochlorite, respectively. These values describe the added chemical mass only; the experiment did not directly measure free residual chlorine after mixing.

To strengthen the quantitative interpretation, the repeated measurements were summarized using the arithmetic mean, sample standard deviation (SD), range, and coefficient of variation (CV = SD/mean x 100%). These statistics were calculated from the original tabulated values and do not introduce new experimental measurements.

Table 1. Main System Components and Functions

Component	Function
Omron CP1H-XA40DR-A PLC	Executes sequence logic, timers, and actuator output commands
START/OFF/STOP push buttons	Provide operator commands to initiate, terminate, or interrupt operation
Relay interfaces	Electrically switch the three pumps and mixer from PLC outputs
Pump 1	Transfers source water to the treatment vessel
Pump 2	Adds prepared calcium hypochlorite solution
Mixer motor	Mixes water and treatment chemical
Pump 3	Transfers the treated batch to the downstream container
Wonderware InTouch HMI	Displays actuator and command-state information for supervisory monitoring

3. Result and Discussion

3.1 Prototype Realization and Functional Logic

The completed prototype integrates the PLC, relay interfaces, pumps, mixer, treatment vessels, and local computer-based HMI in a single laboratory-scale setup. The electrical wiring and ladder implementation provide a direct mapping between command inputs and actuator outputs. Functional testing showed that all six tested command-state combinations produced the intended final state. The START command activated the system from OFF and maintained operation when already ON; OFF deactivated an operating system and maintained the OFF state when already inactive; and STOP changed an active system to the stopped state while leaving an already inactive system unchanged. Thus, the observed functional success rate was 6/6 (100%) for the tested scenarios.

This result supports the principal objective of replacing manual one-by-one actuator operation with deterministic sequence control. Similar PLC-SCADA studies have emphasized the value of deterministic logic, centralized visualization, and rapid fault/state awareness for treatment processes [1]. However, the

ISSN 3025-3780 (online)
ISSN 3025-4590 (printed)

present prototype is deliberately simpler than full-scale systems because the actuator sequence is timer based and does not yet use analog process feedback such as level, flow, pH, turbidity, or residual chlorine.

Fig. 5 Fabricated PLC-based water-treatment automation prototype

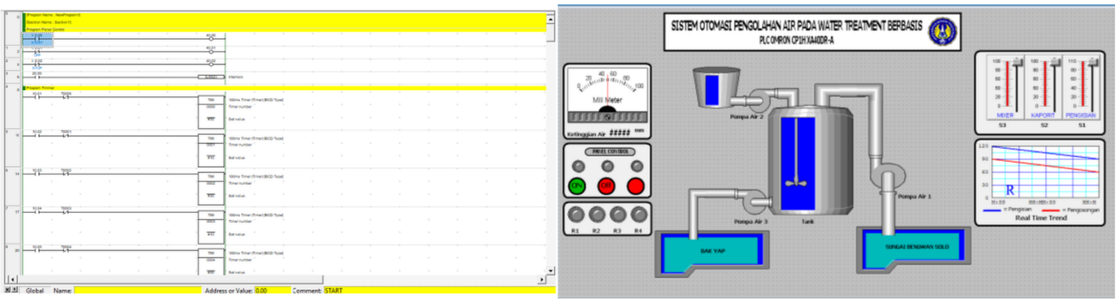

(a) PLC ladder program

(b) SCADA/HMI monitoring

Fig. 6 Implemented control and monitoring software: (a) PLC ladder program and (b) SCADA/HMI display

Table 2. Functional Command-State Verification

No.	Command	Initial state	Final state	Interpretation
1	ON	OFF	ON	System operates
2	OFF	ON	OFF	System turns off
3	STOP	ON	OFF	System stops temporarily
4	ON	ON	ON	System remains operating
5	STOP	OFF	OFF	System remains stopped
6	OFF	OFF	OFF	System remains off
6	OFF	OFF	OFF	System remains off

3.2 Batch Filling Repeatability

Across ten filling cycles, water height varied from 10.5 to 10.9 cm, with a mean of 10.72 cm and an SD of 0.13 cm. The corresponding batch volume ranged from 2.190 to 2.273 L, with a mean of 2.236 L and an SD of 0.027 L. The coefficients of variation were 1.23% for height and 1.22% for volume. These relatively small variations indicate that the timer-based filling stage was repeatable under the tested laboratory conditions.

The repeatability result is useful because the original design does not include closed-loop level sensing. In a timer-based system, stable pump characteristics and hydraulic conditions are required to maintain consistent volume. Recent water-treatment monitoring studies increasingly incorporate online sensing precisely to reduce dependence on fixed timing and to provide direct process feedback [3]-[5]. Therefore, the observed CV of approximately 1.2% should be interpreted as a baseline under the tested setup rather than evidence that timer control will remain equally consistent under changing head pressure, pump wear, or supply-voltage variation.

Table 3. Repeated Filling Test and Descriptive Statistics

Trial	Water height (cm)	Volume (L)
1	10.9	2.273
2	10.7	2.232
3	10.8	2.253
4	10.6	2.211
5	10.8	2.253
6	10.7	2.232
7	10.6	2.211
8	10.5	2.190
9	10.7	2.232
10	10.9	2.273
Mean	10.72	2.236
SD	0.13	0.027
CV (%)	1.23	1.22

3.3 HMI/SCADA Response Performance

The response time between the physical/command event and the corresponding HMI indication ranged from 0.2 to 1.0 s. The fastest response was observed for the STOP indicator (0.2 s), while the slowest was observed for Pump 3 (1.0 s). The mean response time across the seven monitored components was 0.543 s with an SD of 0.282 s and a median of 0.5 s. All observed responses were at or below 1 s.

For a laboratory supervisory interface, this response is adequate for visual state monitoring because the process sequence itself operates on much longer pump and mixing intervals. The result also confirms that the Wonderware InTouch display was synchronized with the PLC sufficiently for operator observation. Nevertheless, this test characterizes only the local prototype configuration and should not be generalized to networked or remote SCADA deployments. Modern water-treatment digitalization platforms place additional emphasis on time synchronization, data pipelines, anomaly detection, and remote communication reliability [6]-[10]. Future evaluation should therefore distinguish PLC scan time, communication delay, HMI refresh rate, and end-to-end event latency.

Table 4. HMI Response-Time Measurements

Component / indicator	Observed state	Response time (s)
Pump 1	ON indication	0.5
Pump 2	ON indication	0.8
Pump 3	ON indication	1.0
Mixer	Rotating indication	0.3
START lamp	ON	0.6
OFF lamp	ON	0.4
STOP lamp	ON	0.2
Mean ± SD	-	0.543 ± 0.282

3.4 Calcium hypochlorite screening and water-quality interpretation

At the calculated calcium hypochlorite mass of 4.44 mg per 2 L batch, all ten reported observations were colorless and showed no detectable odor or taste. At 13.33 mg per 2 L, all ten observations remained colorless, but five of ten were reported to have a slight chlorine odor and five of ten were reported to have a slight bitter taste. These counts correct an inconsistency in the narrative of the original manuscript, which stated six odor events and four taste events even though the tabulated observations correspond to five and five, respectively. The higher nominal dose therefore produced more frequent sensory changes under the reported test conditions.

The water-quality conclusion requires important qualifications. The applied chemical mass does not equal the free residual chlorine concentration after treatment because chlorine demand, contact time, mixing, temperature, organic matter, and other water characteristics affect residual disinfectant [18], [19]. Consequently, the organoleptic observations cannot establish microbiological safety or compliance with drinking-water standards. Recent research on chlorine management emphasizes direct residual monitoring and optimization rather than inferring treatment adequacy from the applied dose alone [18], [19]. The present results should therefore be described as dose-response screening of color, odor, and taste, not as proof that the produced water is safe for consumption.

A stronger next-stage design would add a residual-chlorine sensor together with pH and turbidity measurements and use these signals as interlocks or feedback variables. This would move the prototype from open-loop sequencing toward sensor-informed or closed-loop dosing. Comparable trends are visible in recent studies that use real-time soft sensors, predictive models, and advanced control to adjust chemical addition according to changing process conditions [14]-[17], [20].

ISSN 3025-3780 (online)
ISSN 3025-4590 (printed)

Table 5. Summary of Organoleptic Observations for Two Calcium Hypochlorite Doses (n = 10 per Condition)

$Ca(OCl)_2$ mass / 2 L	Nominal dose	No detectable odor	No detectable taste	Colorless
4.44 mg	2 mg/L	10/10	10/10	10/10
13.33 mg	6 mg/L	5/10	5/10	10/10
13.33 mg	6 mg/L	5/10	5/10	10/10

Note: At 13.33 mg, slight chlorine odor was reported in 5/10 observations and slight bitter taste in 5/10 observations. These are sensory observations, not residual-chlorine measurements.

3.5 Limitations and development pathway

The main limitation of this study is that the system was evaluated as a laboratory prototype with a small number of repeated cycles and a timer-based process sequence. The experiment did not quantify flow rate, energy consumption, PLC scan time, pump duty variation, alarm recovery, network robustness, or long-duration reliability. Water quality was not characterized using standard analytical measurements such as pH, turbidity, free residual chlorine, total dissolved solids, or microbiological indicators. These limitations restrict the conclusions to automation functionality, HMI responsiveness, filling repeatability, and descriptive organoleptic observations.

Despite these limitations, the prototype provides a useful engineering baseline for staged development. The next version should incorporate level or flow sensing for volume control, pH and turbidity sensing for process supervision, residual-chlorine measurement for dosing validation, data logging for traceability, and fault/alarm handling for pumps and communication links. Once these variables are available, the system can be extended toward adaptive dosing, predictive maintenance, or digital-twin functions such as those reported in recent water-treatment research [2], [6]-[10].

4. Conclusion

A laboratory-scale water-treatment automation system based on an Omron CP1H-XA40DR-A PLC and Wonderware InTouch SCADA was successfully implemented and evaluated. All six functional command-state tests produced the intended response, while the HMI displayed system changes with a mean response time of 0.543 ± 0.282 s and a maximum observed delay of 1.0 s. Ten repeated filling cycles produced a mean water height of 10.72 ± 0.13 cm and a mean batch volume of 2.236 ± 0.027 L, with CV values close to 1.2%, indicating good repeatability under the tested laboratory conditions. Calcium hypochlorite screening showed no reported odor, taste, or color change at 4.44 mg per 2 L, whereas the 13.33 mg dose produced slight odor and/or bitter taste in half of the observations while remaining colorless. These water-quality observations are not sufficient to establish drinking-water safety because residual chlorine and standard physicochemical and microbiological parameters were not measured. The main contribution of this work is therefore the validated low-complexity PLC-SCADA automation layer and its quantitative baseline performance. Future development should replace timer-only operation with level/flow feedback, add pH, turbidity, and residual-chlorine sensors, implement alarm and data-logging functions, and evaluate closed-loop dosing and long-term reliability.

Author Contribution:

Please complete the author-contribution statement before submission.

Funding:

Please verify and complete the funding statement before submission.

Acknowledgment:

Please complete this section if applicable.

Conflicts of Interest:

Please confirm and complete the conflict-of-interest statement before submission.

References

[1] K. H. Kaittan and S. J. Mohammed, "PLC-SCADA automation of inlet wastewater treatment processes: Design, implementation, and evaluation," Journal Europeen des Systemes Automatises, vol. 57, no. 3, pp. 787-796, 2024, doi: 10.18280/jesa.570317.

[2] S. Cairone et al., "Revolutionizing wastewater treatment toward circular economy and carbon neutrality goals: Pioneering sustainable and efficient solutions for automation and advanced process control with smart and cutting-edge technologies," Journal of Water Process Engineering, vol. 63, Art. no. 105486, 2024, doi: 10.1016/j.jwpe.2024.105486.

[3] A. Moretti, H. L. Ivan, and J. Skvaril, "A review of the state-of-the-art wastewater quality

characterization and measurement technologies. Is the shift to real-time monitoring nowadays feasible?," Journal of Water Process Engineering, vol. 60, Art. no. 105061, 2024, doi: 10.1016/j.jwpe.2024.105061.

[4] H. M. Forhad et al., "IoT based real-time water quality monitoring system in water treatment plants (WTPs)," Heliyon, vol. 10, no. 23, Art. no. e40746, 2024, doi: 10.1016/j.heliyon.2024.e40746.

[5] M. A. Murti et al., "Smart system for water quality monitoring utilizing long-range-based Internet of Things," Applied Water Science, vol. 14, Art. no. 69, 2024, doi: 10.1007/s13201-024-02128-z.

[6] C. Rodriguez-Alonso, I. Pena-Regueiro, and O. Garcia, "Digital twin platform for water treatment plants using microservices architecture," Sensors, vol. 24, no. 5, Art. no. 1568, 2024, doi: 10.3390/s24051568.

[7] S. Daneshgar et al., "A full-scale operational digital twin for a water resource recovery facility-A case study of Eindhoven Water Resource Recovery Facility," Water Environment Research, vol. 96, no. 3, Art. no. e11016, 2024, doi: 10.1002/wer.11016.

[8] Y. Wei, A. W.-K. Law, and C. Yang, "Real-time data-processing framework with model updating for digital twins of water treatment facilities," Water, vol. 14, no. 22, Art. no. 3591, 2022, doi: 10.3390/w14223591.

[9] Y. Wei, A. W.-K. Law, C. Yang, and D. Tang, "Combined anomaly detection framework for digital twins of water treatment facilities," Water, vol. 14, no. 7, Art. no. 1001, 2022, doi: 10.3390/w14071001.

[10] Z. Ma et al., "Towards the digitalization of water treatment facilities: A case study on machine learning-enabled digital twins," Journal of Water Process Engineering, vol. 77, Art. no. 108316, 2025, doi: 10.1016/j.jwpe.2025.108316.

[11] J.-H. Wang et al., "An online intelligent management method for wastewater treatment supported by coupling data-driven and mechanism models," Journal of Water Process Engineering, vol. 53, Art. no. 103653, 2023, doi: 10.1016/j.jwpe.2023.103653.

[12] K. J. Nam, S. K. Heo, S. Y. Kim, and C. K. Yoo, "A multi-agent AI reinforcement-based digital multi-solution for optimal operation of a full-scale wastewater treatment plant under various influent conditions," Journal of Water Process Engineering, vol. 52, Art. no. 103533, 2023, doi: 10.1016/j.jwpe.2023.103533.

[13] M. V. Ruano, J. Ribes, A. Ruiz-Martinez, A. Seco, and A. Robles, "An advanced control system for nitrogen removal and energy consumption optimization in full-scale wastewater treatment plants," Journal of Water Process Engineering, vol. 57, Art. no. 104705, 2024, doi: 10.1016/j.jwpe.2023.104705.

[14] H. Ding et al., "Soft sensor enabled real-time chemical dosing control systems for wastewater treatment: From hybrid model to full-scale application," Journal of Water Process Engineering, vol. 63, Art. no. 105431, 2024, doi: 10.1016/j.jwpe.2024.105431.

[15] H. Daraei et al., "DOC signal-based alum dose control for drinking water treatment plants," Journal of Water Process Engineering, vol. 54, Art. no. 103934, 2023, doi: 10.1016/j.jwpe.2023.103934.

[16] S. Lin, J. Kim, C. Hua, M.-H. Park, and S. Kang, "Coagulant dosage determination using deep learning-based graph attention multivariate time series forecasting model," Water Research, vol. 232, Art. no. 119665, 2023, doi: 10.1016/j.watres.2023.119665.

[17] J. Kim et al., "Optimizing coagulant dosage using deep learning models with large-scale data," Chemosphere, vol. 350, Art. no. 140989, 2024, doi: 10.1016/j.chemosphere.2023.140989.

[18] M. Moeini and A. Abokifa, "Chlorine dosage management in drinking water systems: Comparing Bayesian optimization to evolutionary algorithms," Journal of Hydroinformatics, vol. 26, no. 11, pp. 2720-2738, 2024, doi: 10.2166/hydro.2024.090.

[19] Y. Khor, A. R. Abdul Aziz, and S. S. Chong, "Recent developments and sustainability in monitoring chlorine residuals for water quality control: A critical review," RSC Sustainability, vol. 2, no. 9, pp. 2468-2485, 2024, doi: 10.1039/D4SU00188E.

[20] M. Han, J. Yao, A. W.-K. Law, and X. Yin, "Efficient economic model predictive control of water treatment process with learning-based Koopman operator," Control Engineering Practice, vol. 149, Art. no. 105975, 2024, doi: 10.1016/j.conengprac.2024.105975.

JRAEE
Journal of Robotics, Automation, and Electronics Engineering
Vol. 3, No. 1, 2025, pp. 153-164
e-ISSN 3025-3780
https://journal.uny.ac.id/v3/jraee

Non-Invasive Device for Cholesterol, Uric Acid, and Glucose Monitoring: Implementation of Moving Average Filter

Muhammad Falah Ar-Rasid[a,1], Purno Tri Aji[b,2,*]

[a, b]Dept. of Electrical and Electronic Engineering, Vocational Faculty, Universitas Negeri Yogyakarta
[1]muhammadfalah.2020@student.uny.ac.id; [2]purno.tri@uny.ac.id
[*]Corresponding Author

ARTICLE INFO

Article History
Received 12 Mar 2025
Revised 29 Aug 2026
Accepted 31 Aug 2026

ABSTRACT

Early detection is crucial in preventing diseases caused by high blood glucose, cholesterol, and uric acid levels through routine examinations. However, current testing devices are invasive, uncomfortable, complex, and generate medical waste. Therefore, this study aimed to develop and design a non-invasive measurement tool for these three parameters using the MAX30102 sensor. This research applied the Research and Development (R&D) method using the ADDIE model, adapted to the laboratory testing stage. The infrared values measured by the MAX30102 sensor on the fingertip were converted into mg/dL for blood glucose, cholesterol, and uric acid using a linear regression method to form regression equations. The converted data were then compared with standard devices to assess their accuracy. Additionally, a moving average filter was applied to reduce noise, smooth the signal, and balance the response to data changes. The measurement results were displayed on an OLED screen, a smartphone application for monitoring history and providing health information, and a speaker announcing the result categories. The results of the study showed that the cholesterol measurement accuracy was 89.71%, with an error rate of 10.29%, the uric acid accuracy was 92.98%, with an error rate of 7.02%, and the blood glucose accuracy was 92.64%, with an error rate of 7.36%.

Keywords
Programmable logic controller;
SCADA;
Water treatment automation;
Human-machine interface;
Chlorine dosing.

ABSTRAK

Deteksi dini sangat penting untuk mencegah penyakit yang ditimbulkan dari tingginya kadar gula darah, kolesterol, dan asam urat melalui pemeriksaan rutin. Namun, alat pengecekan saat ini bersifat invasive, tidak nyaman, kompleks, dan menghasilkan limbah medis. Sehingga penelitian ini bertujuan untuk mengembangkan dan merancang alat pengukur pada ketiga kadar parameter secara non-invasive dengan sensor MAX30102. Penelitian ini menerapkan R&D dengan model ADDIE yang disesuaikan sampai pengujian laboratorium. Nilai infrared yang diukur oleh sensor MAX30102 pada ujung jari dikonversikan ke dalam bentuk mg/dl pada gula darah, kolesterol dan asam urat dengan metode regresi linier dan membentuk persamaan regresi. Data yang sudah dikonversi akan dibandingkan dengan alat standar untuk dilihat tingkat akurasinya. Selain itu, penulis

ISSN 3025-3780 (online)
ISSN 3025-4590 (printed)

menerapkan moving average filter untuk mengurangi noise, menghaluskan sinyal dan respon perubahan data yang seimbang. Data hasil pengukuran akan ditampilkan pada OLED display, aplikasi smartphone sebagai riwayat monitoring pengukuran dan penyedia informasi kesehatan, serta speaker untuk pembacaan hasil kategori. Berdasarkan hasil penelitian, nilai akurasi kadar kolesterol sebesar 89,71% dengan error 10,29% akurasi asam urat sebesar 92,98% dengan error 7,02% dan akurasi gula darah sebesar 92,64% dengan error 7,36%.

1. Introduction

Non-communicable diseases (NCDs) are types of diseases that cannot be transmitted from sufferers to others, or which are caused by a person's lifestyle, behavior, and are not caused by viruses or bacteria [1]. Another name for NCDs is degenerative diseases. Health conditions in which organs and tissues deteriorate over time due to changes in body cells, which ultimately affect the function of all organs, are called degenerative diseases. Degenerative diseases increase due to decreased physical activity, eating habits, and lifestyle. [2]. Lifestyle changes like this can cause stroke, coronary heart disease, diabetes, and cancer, which can be caused by various factors such as high blood sugar, cholesterol, and uric acid [3]. The results of the 2018 Basic Health Survey (Riskesdas) showed that non-communicable diseases such as diabetes, hypertension, cancer, stroke, and chronic kidney disease increased compared to the 2013 Riskesdas. These results indicate that this disease is increasing. Diabetes increased from 6.9% to 8.5%, hypertension increased from 25.8% to 34.1%, cancer increased from 1.4% to 1.8%, stroke increased from 7% to 10%, and chronic kidney disease increased from 2% to 3.8%, the prevalence of gout (gout arthritis) in Indonesia reached 11.9% [4].

Based on data from the International Diabetes Federation (IDF) 2021, there are 19.5 million people in Indonesia who have diabetes, making it the fifth largest number of diabetes sufferers in the world. High cholesterol is also a serious health problem in Indonesia, 28% of people in Indonesia have high cholesterol.

One way to prevent degenerative diseases is to conduct an initial examination by checking and maintaining normal cholesterol, uric acid, and blood sugar levels, currently being tested invasively. Invasive methods have drawbacks for patients, such as blood and needle phobia, which makes them uncomfortable and causes fear [5]. This process requires the use of needles for blood sampling, the use of 3 different test strip tools to measure the three levels of these parameters and cannot be monitored digitally through the application and still uses paper manually to store medical records [6]. In addition, invasive testing procedures pollute the environment, are potentially harmful and are difficult to decompose because they produce used syringes, used cotton, used test strips which are included in medical waste [7].

Based on these problems, the author will create a system that can determine the three parameters of levels non-invasively. This system only uses one sensor, namely the MAX30102 sensor which is processed by the NodeMCU ESP8266 microcontroller, then in the sensor reading, signal filtering is carried out using a simple moving average filter to reduce noise, smooth the signal, and a balanced response to changes. This system will also be displayed in the form of an OLED display so that it can be seen directly, there is a speaker to emit a sound reading the category of cholesterol, uric acid, and blood sugar measurement results and is based on the internet of things for monitoring and providing information related to health and diseases from cholesterol, uric acid, and blood sugar which are presented in the form of smartphone applications. In this study, the author developed tool entitled Development of a Non-Invasive Cholesterol, Uric Acid, and Blood Sugar Measuring Tool with the Application of Moving Average Filter. The use of non-invasive tools is expected to be a solution for easy medical devices, can provide a sense of comfort and safety, no phobia and fear to patients without having to take blood samples using syringes and does not produce medical waste that can pollute the environment.

2. Methods

2.1 Simple Linear Regression

Regression analysis is a statistical method used to determine the linear functional relationship between a response variable and a predictor variable. When conducting regression analysis, two types of variables are used: the dependent variable (Y), which is the response, and the independent variable (X), which is the predictor. The predictor variable (X) is the variable that influences or explains another variable (Y), and the variable that is influenced or explained by X is called the response variable (Y) [8]. A simple linear regression equation is shown in

$$y = a + bx \tag{1}$$

In there are variables such as the value of y is the estimated dependent variable, while x is the independent variable, a is the intercept, namely the value of y when x = 0, and b is the slope, namely the average change in y against a change in one unit of x. The coefficients a and b are the regression coefficients, these values can be calculated from equations (2) and (3) [9].

$$b = \frac{n(\sum xy) - (\sum x)(\sum y)}{n(\sum x^2) - (nx^2)} \tag{2}$$

$$a = \frac{\sum y - b(\sum x)}{n} \tag{3}$$

2.2 Moving Average Filter

Moving Average Filter (MAF) is a type of data filtering that can be applied in sensor readings, functioning to strengthen signals and reduce noise to achieve better results. This filter system consists of using the average value of a set of data received over a certain period of time. The MAF filter eliminates deviations in the data, thus only taking data with relevant values [10]. Simple Moving Average (SMA) uses a sliding window to take the average over a certain number of time periods.

$$SMA = \frac{data_1 + data_2 + \cdots + data_n}{M} \tag{4}$$

2.3 Design Concept

The Research and Development (RnD) method or research and development is a type of research used to create products and test their effectiveness so that in creating a product, research is carried out in the form of needs analysis and testing the effectiveness of the product so that it can function in society [11].

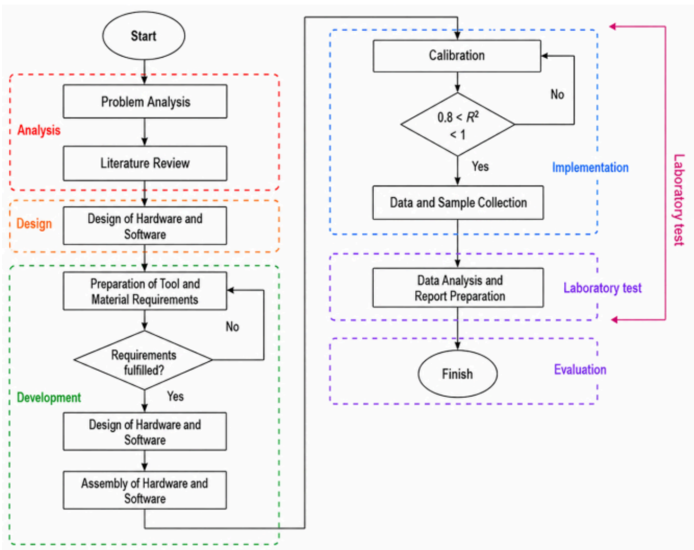

Fig. 1 Research flow chart

In is the ADDIE development model applied in this research which consists of five stages including Analysis, Design, Development, Implementation, and Evaluation. In the Implementation and Evaluation model, there is an adjustment of needs, namely up to laboratory testing.

Journal of Robotics, Automation, and Electronics Engineering
Vol. 3, No. 1, 2025, pp. 153-164
ISSN 3025-3780 (online)
ISSN 3025-4590 (printed)

2.4 System Design Block Diagram

In the design block diagram there are several parts, namely input, process, output and resource blocks.

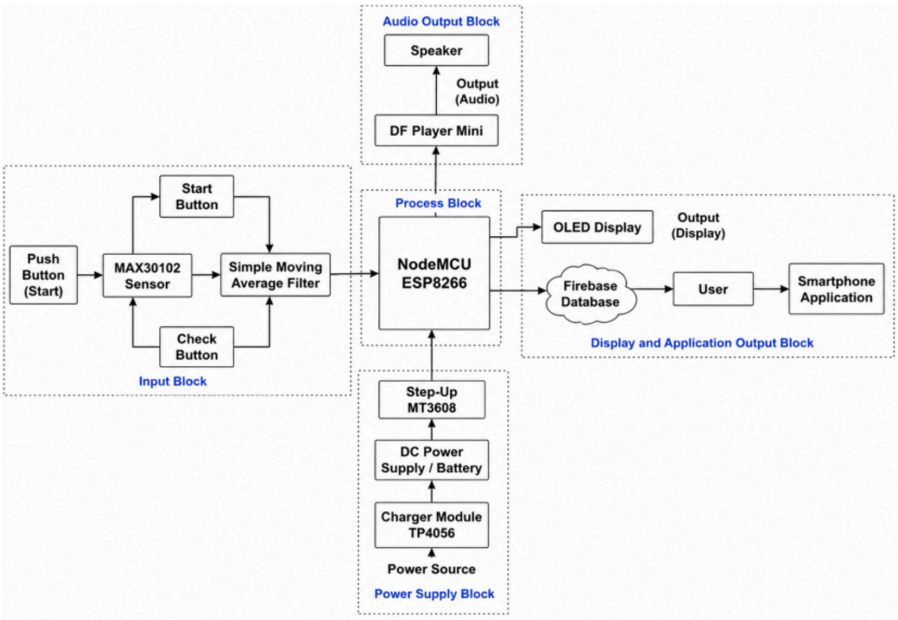

Fig. 2 Block diagram

In the input block section there are fingers, MAX30102 sensors, and start and recheck buttons. Then there is a filter, namely the moving average filter. In the process block section, the ESP8266 microcontroller is used to process IR values to mg/dl units and control input and output. In the output block consisting of an OLED display, speaker, and smartphone application. In the resource block there is a battery, MT3608 step up, and TP4056 charger module.

2.5 Electronic Design

The electronic design of this tool aims to provide an overview or design and connect to each component used, ensure the system can function properly, and facilitate wiring in the circuit. Consists of components such as MAX30102 sensors, ESP8266, Oled display, 2 buttons, DF mini player, mini speaker, battery, TP4056 charger module, and Step up MT3608.

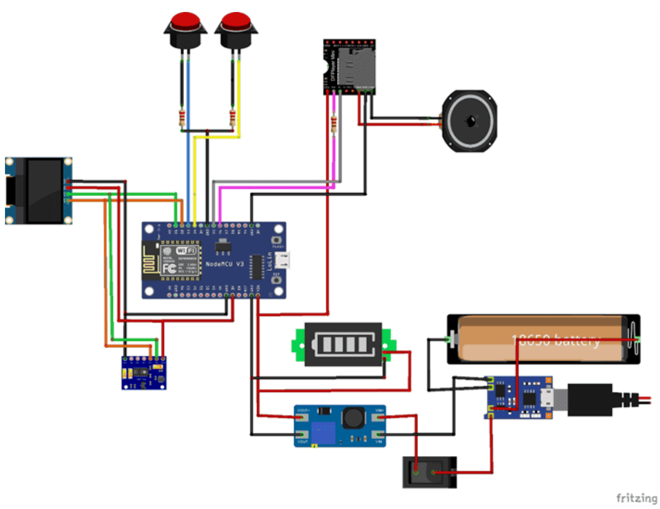

Fig. 3 Electronic design

2.6 NodeMCU ESP8266 Program Design

The program created on the NodeMCU ESP8266 has several main functions, namely reading sensors, processing data, displaying data output results, and WiFi connectivity to send and receive data.

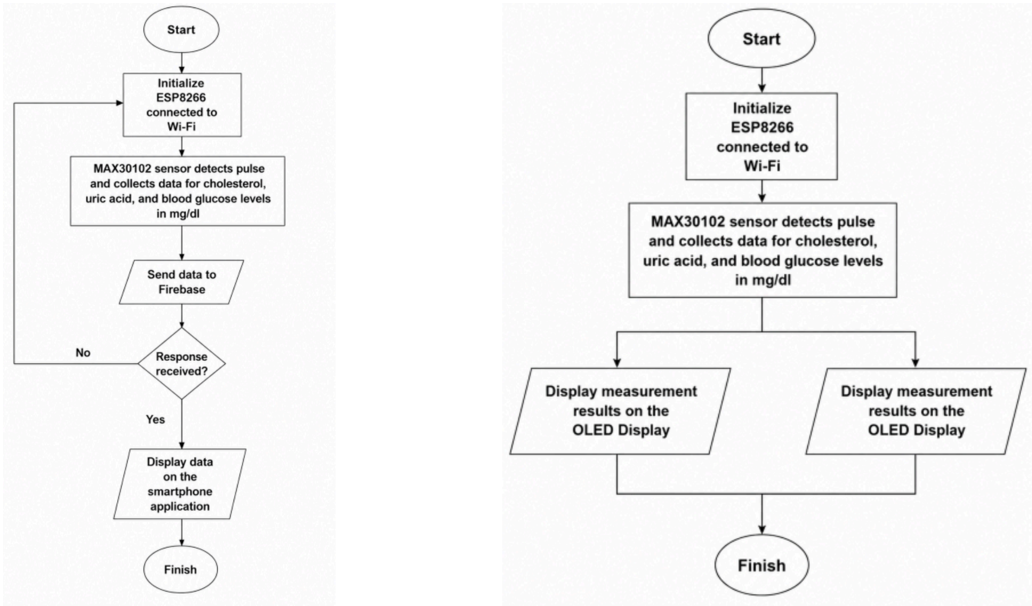

(a) (b)

Fig. 4 (a) Flowchart of ESP8266 design on smartphone application (b) Flowchart of program design on tool prototype

The design of the program on is a design for a smartphone application that begins with the initialization of the esp8226 connected to wifi, then the MAX30102 sensor reads the measurement of the three parameters of levels in mg/dl units then sends the data to firebase which will be displayed on the smartphone application. While on is a program design on the tool prototype that begins when the esp8266 is connected to wifi then the MAX30102 sensor reads the measurement results, then the data results will be displayed on the OLED and emit sound through the speaker for reading the category.

3. Results and Discussion

3.1 Prototype Tool Box and Finger Clip Making Results

The box design measures 12.5cm x 8.5cm with a height of 5cm. Furthermore, the finger clip design is used as a finger placement which contains the MAX30102 sensor, this finger clip functions so that the finger does not easily shift or move, the right finger position, comfort and ease of use.

(a) (b)

Fig. 5 (a) Right view of the tool prototype (b) Left view of the tool prototype

3.2 Moving Average Filter Testing

At the simple moving average filter test stage, it is carried out experimentally by considering the needs. The size of the window size or window size will affect the signal results.

ISSN 3025-3780 (online)
ISSN 3025-4590 (printed)

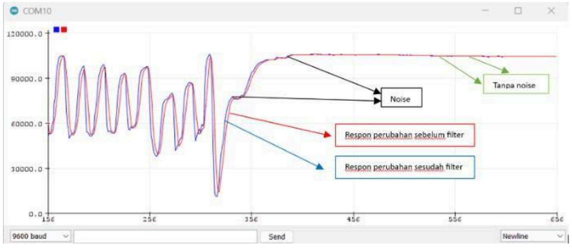

Fig. 6 Signal results with window size 5

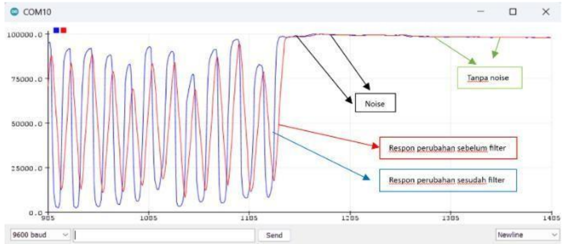

Fig. 7 Signal results with window size 10

Fig. 6 is the result of the signal before being filtered (red) and after being filtered (blue). The signal results have a response that is not so fast in responding to data changes. Then the noise can be reduced and the signal looks smooth. Meanwhile In Figure 7, the response to the change is seen to be delayed, then the noise is seen to be reduced and the signal is smoother. In this study, the author applies a simple moving average filter to reduce noise, smooth the signal, and a balanced data change response. So based on the test results, the author chooses a window size of 5. The filtering process begins with the reading of the MAX30102 sensor in the form of an IR or infrared value. Furthermore, determining the window size 5 means that every time you perform an average calculation, it uses the last data taken from the input.

$$y[5] = \frac{x_1 + x_2 + x_3 + x_4 + x_5}{5} \tag{5}$$

```
//SIMPLE MOVING AVERAGE FILTER
SUM = SUM - READINGS[INDEX];          // Kurangi nilai yang akan digantikan dari total
VALUE = particleSensor.getIR();       // Baca nilai sensor
READINGS[INDEX] = VALUE;              // Simpan nilai sensor di dalam array
SUM = SUM + VALUE;                    // Tambahkan nilai baru ke total
INDEX = (INDEX+1) % WINDOW_SIZE;      // Pindah ke indeks berikutnya, lingkupkan dengan WINDOWS_SIZE
AVERAGED = SUM / WINDOW_SIZE;         // Hitung nilai rata-rata
```

Fig. 8 Initialization of MAF program variables

```
//VARIABEL MOVING AVERAGE FILTER
#define WINDOW_SIZE 5          //Jumlah pembacaan yang akan diratakan
int INDEX = 0;                 //Indeks saat ini dalam array pembacaan
int VALUE = 0;                 //Pembacaan sensor
int SUM = 0;                   //Total pembacaan yang disimpan dalam array
int READINGS[WINDOW_SIZE];     //Array untuk menyimpan nilai pembacaan
int AVERAGED = 0;              //Nilai Rata-rata
```

Fig. 9 MAF program formula

Figure 8 and Figure 9 show the variable initialization and the moving average filter application formula that will be entered into the Arduino IDE program. The order of the average divisor can be changed at the window size value. The IR value from the filter result is then used to convert the three parameter levels.

3.3 Tool Calibration

Calibration of the MAX30102 sensor produces an IR value read from the volunteer's left index finger. The value is obtained from the results of reading the level of light absorbed by the blood in the capillaries at the tip of the finger and the flowing blood will absorb different light depending on its oxygen content. The data collection process begins with blood samples taken using a standard Elvasense 3in1 tool, then using a prototype tool on ten random volunteers. The IR value is compared with the three level parameters. Furthermore, the data is plotted in the form of a graph in Microsoft Excel. Then, the equation of the straight line and the coefficient of determination R^2 can be seen with the Treadline feature.

Fig. 10, Fig. 11, and Fig. 12 show the correlation graphs between the average IR values against the three invasive parameters of cholesterol, uric acid, and blood sugar levels. The linear equation obtained for cholesterol y = 0.0024x - 119.45, coefficient of determination $R^2 = 0.9886$. The equation of the line for uric acid y = 0.0002x - 16.502, with $R^2 = 0.9877$ and the equation of the straight line for blood sugar y = 0.0025x - 164.12 with $R^2 = 0.9597$. The calibration results of cholesterol, uric acid, and blood sugar levels produce coefficient determination values that each have a range of 0.8 to 1 so that the coefficient results obtained during calibration show a very strong correlation.

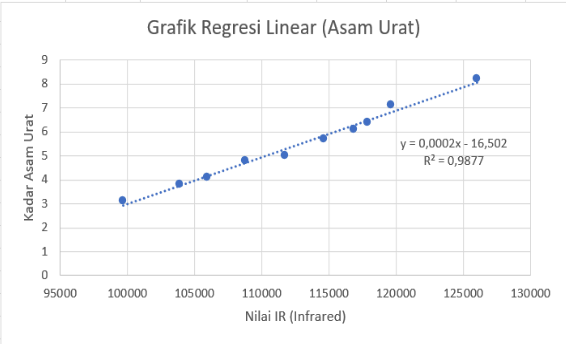

Fig. 10 Linear regression graph of cholesterol compared to IR values

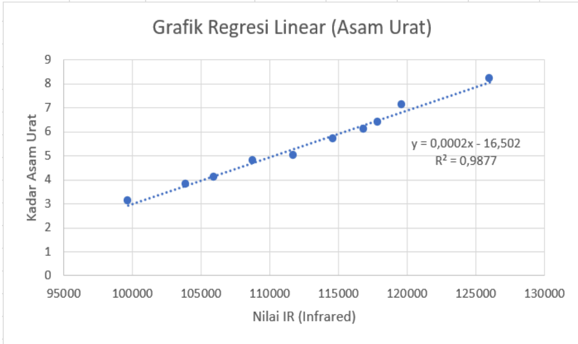

Fig. 11 Linear regression graph of uric acid compared to IR values

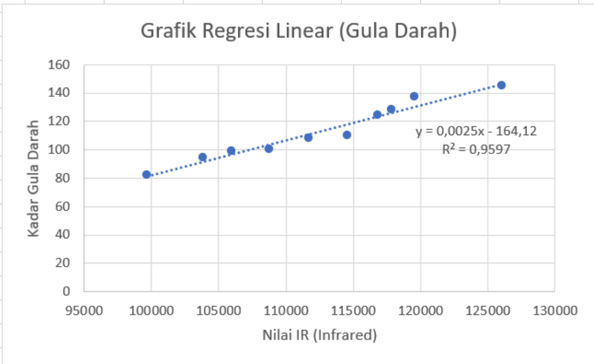

Fig. 12. Linear regression graph of blood sugar compared to IR values

3.4 Precision Testing of Tools

In the precision testing of the prototype of this tool, it was carried out repeatedly 3 times on each volunteer, then the data will be used to calculate the standard deviation, relative error and precision which will be indicators of the precision of the tool.

Table 1. Data from The Results of Precision Testing of The Tool on Cholesterol Levels

Volunter Data			Measurement of the			Average Measurement	Precision Tools (%)
No	**Gender**	**Age**	**1**	**2**	**3**		
1	P	52	167	153	158	159	95,55%
2	L	55	150	145	159	151	95,31%
3	P	22	156	141	143	147	94,45%
4	L	20	131	125	123	126	96,70%
5	L	48	129	116	119	121	94,39%
6	P	51	149	151	133	144	93,16%
7	P	22	169	157	155	160	95,28%
8	L	21	142	129	134	135	95,14%
9	P	50	165	150	153	156	94,91%
10	L	20	142	133	138	138	96,72%
11	L	53	122	124	136	127	94,05%
12	L	42	134	127	123	128	95,65%
13	P	45	176	162	164	167	95,47%
14	P	21	153	144	139	145	95,12%
15	P	23	143	133	136	137	96,26%
16	L	25	142	125	127	131	92,93%
17	P	22	128	138	135	134	96,16%
18	L	22	139	125	124	129	93,52%
19	L	22	138	126	129	131	95,23%
20	P	22	135	140	147	141	95,71%
			Average				**95,09%**

 ISSN 3025-3780 (online)
ISSN 3025-4590 (printed)

Table 2. Data from The Results of Precision Testing of The Tool on Uric Acid Levels

Volunter Data			Measurement of the			Average Measurement	Tools Precision
No	Gen	Age	1	2	3		
1	P	52	7	6,2	6,5	6,6	93,85%
2	L	55	4,5	4,3	4,2	4,3	96,47%
3	P	22	6	5,4	5,7	5,7	94,74%
4	L	20	3,8	4,3	4	4,0	93,76%
5	L	48	3,8	3,4	3,4	3,5	93,46%
6	P	51	5,9	5,3	5,2	5,5	93,07%
7	P	22	6,5	6,9	6,9	6,8	96,59%
8	L	21	4,4	4,9	4,7	4,7	94,61%
9	P	50	5,9	6,8	6,7	6,5	92,37%
10	L	20	4,7	5,3	5	5,0	94,00%
11	L	53	4	3,9	4,1	4,0	97,50%
12	L	42	4,2	4,3	4,2	4,2	98,64%
13	P	45	7,6	7,3	7,2	7,4	97,17%
14	P	21	5,7	5,3	5,8	5,6	95,28%
15	P	23	4,6	4,9	5,1	4,9	94,83%
16	L	25	6,3	6,5	6,4	6,4	98,44%
17	P	22	4,9	4,5	4.7	4,7	93,98%
18	L	22	3,9	4,4	4,2	4,2	93,96%
19	L	22	4,2	4,5	4.4	4,4	95,12%
20	P	22	5,3	5,5	5,1	5,3	96,23%
			Average				**95,20%**

Table 3. Data from The Results of Precision Testing of The Tool on Blood Sugar Levels

Volunter Data			Measurement of the			Average Measurement	Tools Precision
No	Gen	Age	1	2	3		
1	P	52	122	134	123	126	94,73%
2	L	55	101	93	93	96	95,17%
3	P	22	118	110	112	113	96,33%
4	L	20	93	95	89	92	96,69%
5	L	48	95	82	81	86	90,92%
6	P	51	104	109	118	110	93,57%
7	P	22	126	135	121	127	94,43%
8	L	21	108	100	95	101	93,51%
9	P	50	118	119	133	123	93,20%
10	L	20	99	107	106	104	95,81%
11	L	53	88	95	94	92	95,90%
12	L	42	118	130	122	123	95,05%
13	P	45	130	141	134	135	95,88%
14	P	21	120	109	103	111	92,21%
15	P	23	106	105	99	103	96,34%
16	L	25	101	95	96	97	96,70%
17	P	22	108	96	97	100	93,36%
18	L	22	98	90	94	94	95,74%
19	L	22	100	96	93	96	96,35%
20	P	22	111	104	107	107	96,73%
							94,93 %

Based on the results of the prototype measurement data, the average precision value of cholesterol levels was 95.09%, uric acid was 94.93%, and blood sugar was 95.20%. In cholesterol and blood sugar, the tool is stable because the precision value of the tool is appropriate, namely more than 95% [9]. This means that the measuring tool used is stable and consistent and this tool provides results that are almost always the same in repeated measurements. While in uric acid levels, it shows that the tool tends to provide stable results every time a measurement is taken because it is close to 95%.

3.5 Tool Accuracy Testing

The accuracy testing of the prototype tool was tested by comparing it to a standard measuring tool. Data was collected from 20 volunteers randomly. The data collection process was carried out by taking blood samples using the Elvasense 3in1 standard tool once for all three parameters, followed by data collection using a prototype that had been averaged from 3 measurements. Table 4 is the measurement result on the prototype tool and standard tool.

Table 4. Comparison of Measurement Results on The Prototype Tool and Standard Tool

Prototype Measurement Tool	Standard Tool Measurement
	

Next, the error calculation, average percentage error, and accuracy level are carried out using Eq. 6, 7, and 8. Then the results are presented in table 5, table 6, table 7.

$$Error = \frac{abs(actual\ value - data\ testing(training\ data))}{actual\ value} \tag{6}$$

$$Average\ error = \frac{\sum_{i=1}^{n} error\ perhitungan}{banyaknya\ data} \tag{7}$$

$$Accuracy = 100\% - \%\ total\ error \tag{8}$$

Table 5. Data on The Results of The Percentage of Error and Accuracy in Cholesterol Levels

No	Tool Standard	*Tool Prototype*	Error (%
1	147	159	8,16
2	182	151	17,03
3	134	147	9,70
4	118	126	6,78
5	163	121	25,77
6	144	144	0,00
7	148	160	8,11
8	129	135	4,65
9	123	156	26,83
10	139	138	0,72
11	126	127	0,79
12	159	128	19,50
13	198	167	15,66
14	140	145	3,57
15	124	137	10,48
16	131	131	0,00
17	154	134	12,99
18	155	129	16,77
19	156	131	16,03
20	138	141	2,17
Average Percentage Error			**10,29**
Accuracy Level			**89,71%**

Journal of Robotics, Automation, and Electronics Engineering
Vol. 3, No. 1, 2025, pp. 153-164
ISSN 3025-3780 (online)
ISSN 3025-4590 (printed)

Table 6. Data on The Results of The Percentage of Error and Accuracy in Uric Acid Levels

No	Standard Tool	Tool Prototype	Error (%
1	6,2	6,7	8,06
2	4,1	4,3	4,88
3	6,1	5,7	6,56
4	3,8	4	5,26
5	3,1	3,5	12,90
6	7,1	5,5	22,54
7	7,1	6,8	4,23
8	4,7	4,7	0,00
9	6,4	6,5	1,56
10	5	5	0,00
11	3,5	4	14,29
12	4	4,2	5,00
13	6,2	7,4	19,35
14	5,7	5,6	1,75
15	4,8	4,9	2,08
16	7	5,4	22,86
17	4,4	4,7	6,82
18	4,3	4,2	2,33
19	4,4	4,4	0,00
20	5,3	5,3	0,00
Average Percentage Error			**7,02**
Accuracy Level			**92,98%**

Table 7. Data on The Results of The Percentage of Error and Accuracy in Blood Sugar Levels

No	Standard Tool	Tool Prototype	Error (%)
1	128	126	1,56
2	96	96	0,00
3	110	113	2,73
4	95	92	3,16
5	94	86	8,51
6	104	110	5,77
7	124	127	2,42
8	108	101	6,48
9	145	123	15,17
10	99	104	5,05
11	99	92	7,07
12	147	123	16,33
13	137	135	1,46
14	82	111	35,37
15	103	103	0,00
16	100	97	3,00
17	100	100	0,00
18	95	94	1,05
19	102	96	5,88
20	145	107	26,21
Average Percentage Error			**7,36**
Accuracy Level			**92,64%**

Table 5, table 6, and table 7 are the results of the comparison between standard measurements with the prototype of the tool on cholesterol, uric acid, and blood sugar levels obtained from calculations using equations 9, equation 10, equation 11. The accuracy results on cholesterol levels are 89.71% with a percentage error of 10.29%. Then the accuracy results on uric acid levels are 92.98% with a percentage error of 7.02%. Furthermore, the accuracy results on blood sugar levels are 92.64% with a percentage error of 7.36%.

3.6 Smartphone Application

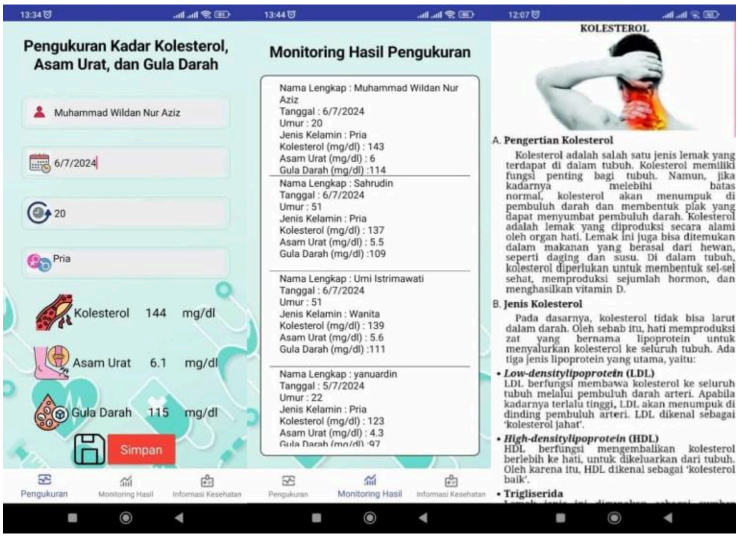

Fig. 13 Display of measurement result monitoring

As shown in Figure 13, users are required to enter their personal information before initiating the measurement. During the measurement process, the results are automatically displayed on the smartphone application. Once the results are displayed, users can save the measurement data by pressing the Save button. The recorded measurement results enable users to monitor their measurement history and may serve as a reference for the early detection of potential health conditions and for determining appropriate follow-up actions. Furthermore, the application provides health-related information, including definitions, causes, prevention and treatment methods, classifications, and other relevant information concerning cholesterol, uric acid, and blood glucose. This feature facilitates users' access to relevant health information and supports a better understanding of these health conditions.

4. Conclusion

The development and manufacture of a non-invasive cholesterol, uric acid, and blood sugar measuring device has been successfully made, functions well, and can be used and the prototype of this tool has the advantages of being easy to use, practical, portable, provides a sense of comfort, safety, and does not produce medical waste and the application of a moving average filter with a window size of 5 can help the sensor reduce noise, smooth the signal, and respond to balanced data changes.

The results of the precision test of the tool are quite stable, namely for cholesterol of 95.09%, uric acid 95.20%, and blood sugar levels of 94.93%. The prototype cannot yet be applied as a standard Health measuring tool because it must have an accuracy of ≥95%. While the prototype of this tool has an accuracy of 89.71% for cholesterol with an error of 10.29%. For uric acid, the accuracy is 92.98% with an error of 7.02% and for blood sugar, the accuracy is 92.64% with an error of 7.36%. However, it has a large enough possibility and prospect to determine the levels of the three parameters. The IoT system and smartphone applications can run well according to their functions, such as monitoring measurement history and providing health information.

Author Contribution:

Muhammad Falah Ar-Rasid: developed the hardware and software system, data collection, data analysis, interpretation of the results, and prepared the initial manuscript. Purno Tri Aji: preparation of the manuscript, and review and revision of the manuscript.

Funding:

This research received no external funding.

Journal of Robotics, Automation, and Electronics Engineering
Vol. 3, No. 1, 2025, pp. 153-164
ISSN 3025-3780 (online)
ISSN 3025-4590 (printed)

Acknowledgment:

The authors would like to thank all parties who provided support and assistance during the implementation of this research.

Conflicts of Interest:

The authors declare no conflict of interest.

References

[1] Tim Promkes RSST, "Penyakit tidak menular (PTM)," Kementerian Kesehatan Republik Indonesia, Jul. 31, 2022. [Online]. Available: Kementerian Kesehatan RI – Penyakit Tidak Menular (PTM).

[2] Amila, E. Sembiring, and N. Aryani, "Deteksi dini dan pencegahan penyakit degeneratif pada masyarakat wilayah Mutiara Home Care," Jurnal Kreativitas Pengabdian Kepada Masyarakat (PKM), vol. 4, no. 1, pp. 102–112, 2021, doi: 10.33024/jkpm.v4i1.3441.

[3] M. R. Kurniawan and A. Humaedi, "Gambaran kesehatan glukosa darah, kolesterol dan asam urat pada guru dan karyawan SDN Cawang," JPKMI (Jurnal Pengabdian Kepada Masyarakat Indonesia), vol. 1, no. 3, pp. 176–185, 2020, doi: 10.36596/jpkmi.v1i3.70.

[4] Badan Penelitian dan Pengembangan Kesehatan, Laporan Nasional Riskesdas 2018. Jakarta, Indonesia: Lembaga Penerbit Badan Penelitian dan Pengembangan Kesehatan, 2019.

[5] N. Yuniar, "Rancang bangun alat deteksi kadar kolesterol dalam darah dengan teknik non-invasive berbasis mikrokontroler Wemos D1 R1," undergraduate thesis, Fakultas Matematika dan Ilmu Pengetahuan Alam, Universitas Lampung, Bandar Lampung, Indonesia, 2023.

[6] D. Sutarya, "Sistem monitoring kadar gula darah, kolestrol dan asam urat secara non-invasive menggunakan sensor GY-MAX 30100," JOULE: Jurnal Ilmiah Teknologi Energi, Teknologi Media Komunikasi dan Instrumentasi Kendali, vol. 1, no. 1, pp. 25–34, 2021.

[7] B. Julia, "Desain dan pengembangan alat ukur kadar hemoglobin dalam darah secara non-invasive menggunakan sensor TCRT5000 berdasarkan prinsip zero waste," undergraduate thesis, Universitas Islam Negeri Walisongo Semarang, Semarang, Indonesia, 2022.

[8] W. Sulistiyowati and C. C. Astuti, Buku Ajar Statistika Dasar. Sidoarjo, Indonesia: UMSIDA Press, 2017, doi: 10.21070/2017/978-979-3401-73-7. [9] T. Nurmar'atin, "Deteksi kadar kolesterol dalam darah secara non-invasive menggunakan sistem telemedika berbasis IoT," undergraduate thesis, Universitas Islam Negeri Walisongo Semarang, Semarang, Indonesia, 2021.

[10] D. R. Tisna and T. Maharani, "Penerapan digital moving average filter pada sensor dissolved oksigen untuk mengukur kualitas air," Journal of Electrical, Electronic, Mechanical, Informatic and Social Applied Science, vol. 1, no. 2, pp. 32–40, 2022, doi: 10.58991/eemisas.v1i2.13.

[11] Sugiyono, Metode Penelitian Kuantitatif, Kualitatif dan R&D. Bandung, Indonesia: Alfabeta, 2013.